OPTIMIZATION AND SENSITIVITY STUDIES OF FLIGHT-PATH TRAJECTORIES

NASA Contract Number NSG 1101
Task Order No. 8

Final Report

Submitted to:

R. M. Hueschen
Mail Stop 473
NASA Langley Research Center
Hampton, Virginia 23365

Submitted by:

Gerald Cook
Principal Investigator

Richard M. Witt

SCHOOL OF ENGINEERING AND APPLIED SCIENCE

RESEARCH LABORATORIES FOR THE ENGINEERING SCIENCES

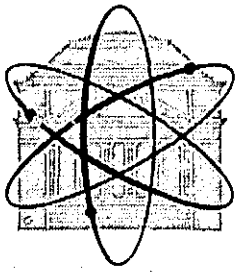

UNIVERSITY OF VIRGINIA
CHARLOTTESVILLE, VIRGINIA 22901

Report No. EE-4038-102-75
September 1975

OPTIMIZATION AND SENSITIVITY STUDIES OF FLIGHT-PATH TRAJECTORIES

NASA Contract Number NSG 1101
Task Order No. 8

Final Report

Submitted to:

R. M. Hueschen
Mail Stop 473
NASA Langley Research Center
Hampton, Virginia 23365

Submitted by:

Gerald Cook
Principal Investigator

Richard M. Witt

Department of Electrical Engineering
RESEARCH LABORATORIES FOR THE ENGINEERING SCIENCES
SCHOOL OF ENGINEERING AND APPLIED SCIENCE
UNIVERSITY OF VIRGINIA
CHARLOTTESVILLE, VIRGINIA

Proposal No. EE-4038-102-75
September 1975

Copy No. 4

I. INTRODUCTION

This report covers our second year of effort on the task of optimizing landing trajectories of the Boeing 737. The primary consideration here is the noise delivered to the population residing near the air terminal but passenger comfort, fuel consumption and time elapsed during the maneuver are also considered.

The results of our efforts during the first year were (1) a digital simulation of the aircraft, (2) a noise model and (3) a passenger comfort model. During the second year, (1) the digital simulation has been made more efficient time-wise, (2) a population model for the Newport News-Hampton area has been developed (3) the noise model has been integrated with the population model, (4) the steepest descent optimization algorithm has been programmed and is in the process of being de-bugged and (5) some constant glide slope trajectories into Patrick Henry Airport at Newport News have been simulated, evaluated with respect to the performance index and their ground track plotted.

II. COMPLETION OF POPULATION MODEL

In our landing-trajectory optimization study, one of the most important considerations is aircraft noise. The noise term in the performance index is based on the number of people receiving objectionable noise and the duration of this noise. The noise model generates the "footprint" of the aircraft. This area then must be weighted with its corresponding population density.

The work on the population model was begun a year ago and was reported in U.Va. Report No. EE-4038-101-74 [1]. The model has now been completed. For completeness the methodology utilized will be reviewed here.

The Newport News-Hampton area was selected as the first site for which to calculate optimal landing trajectories. Data on population were obtained from the U. S. Department of Commerce, Bureau of the Census. These data were in the form of maps with numbers assigned to each city block and to other types of bounded regions. Tables were available which permitted one to look up the population in each of these regions. These regions were of various sizes and shapes, thus necessitating some preprocessing of the data before storing it in the computer. Figures 2.1 through 2.3 illustrate the form of the data.

The approach utilized was to place over the population map a transparent sheet on which had been drawn a grid of rectangles each one having an area of one square mile. All the blocks or regions inside a rectangle were tabulated, the corresponding populations determined and a final total calculated for this rectangle. In this manner the population data were converted to numbers on a uniform grid. This obviously is much more suited to the optimization procedure than the original data format. Figure 2.4 illustrates the technique.

The task was performed manually. To give an idea of the amount of work involved, an area of 20 miles radius contains 1257 square miles. This means for a typical "near terminal area," the population must be tabulated and totaled for 1257 rectangles. Within each rectangle there may be as many as 100 blocks and or regions with the average being approximately 30.

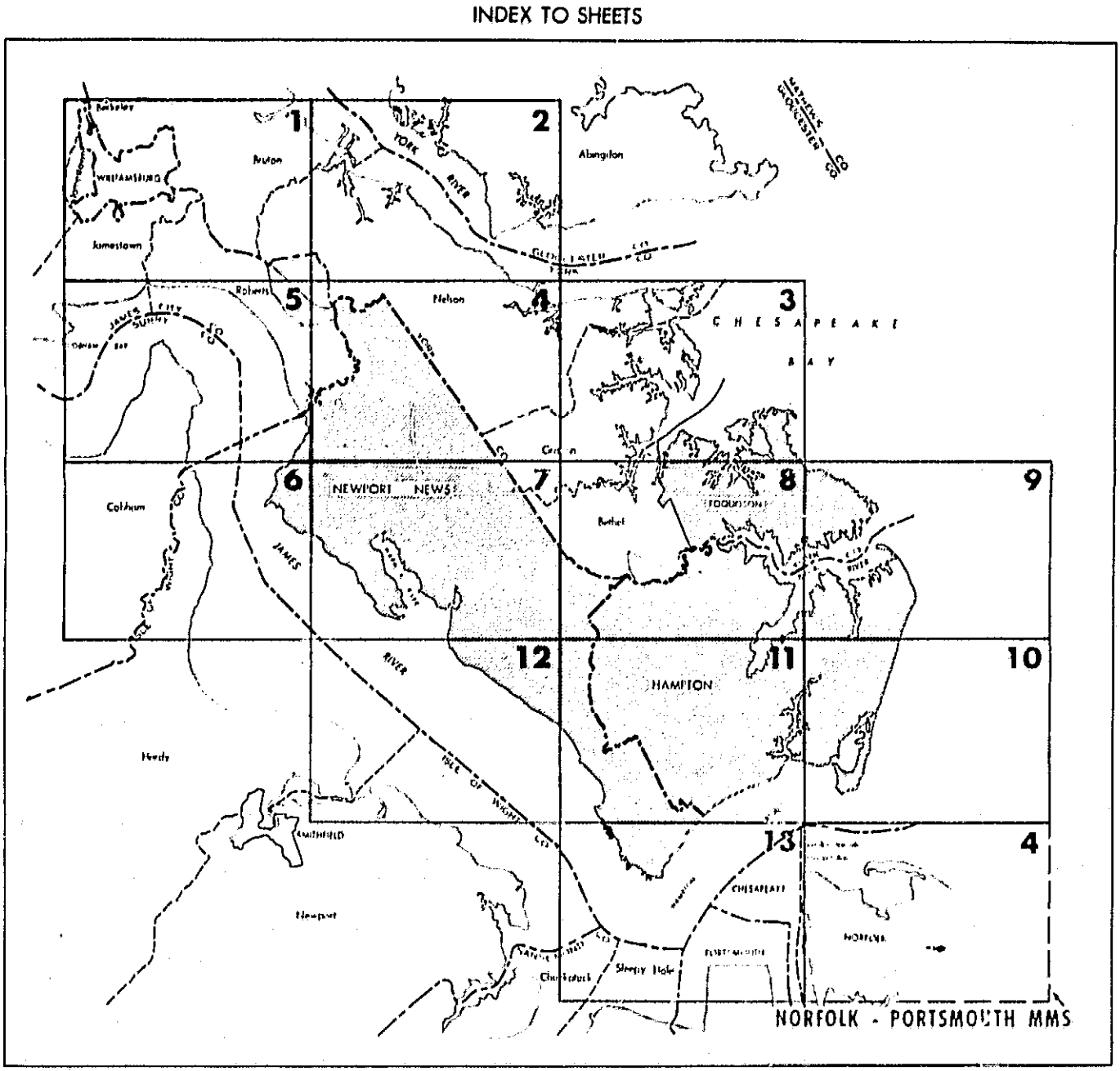

Figure 2.1 An Aggregate of Census Maps for the Newport News-Hampton Area

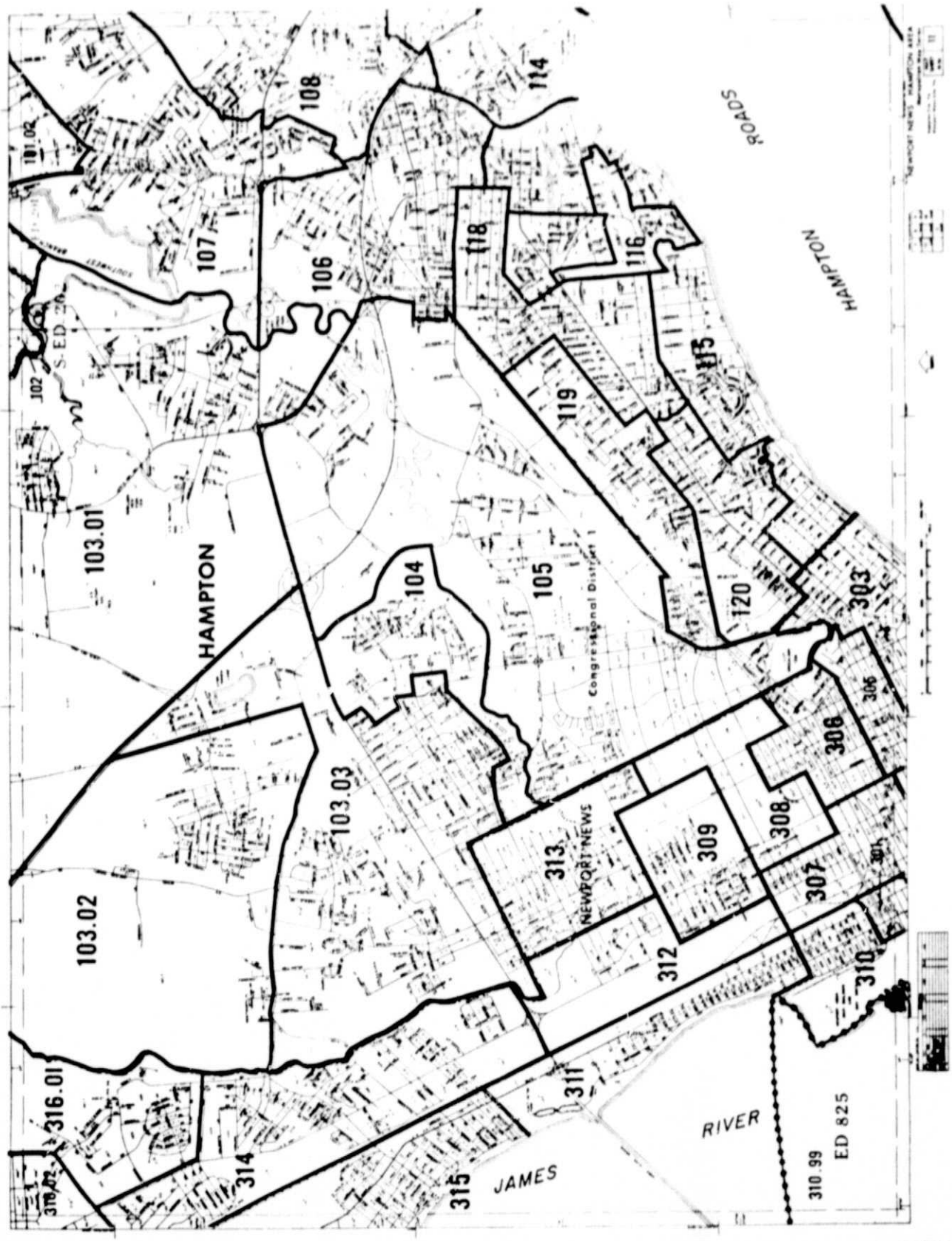

Figure 2.2 Census Map for Region II of the Newport News-Hampton Area

Table 2. **Characteristics of Housing Units and Population, by Blocks: 1970**—Con.

Hampton City

[Data exclude vacant seasonal and vacant migratory housing units. For minimum base for derived figures (percent, average, etc.) and explanation of symbols, see text]

Blocks Within Census Tracts	Total population	Percent of total population: Negro	In group quarters	Under 18 years	65 years and over	Year round housing units: Total	Lacking some or all plumbing facilities	Units in—: One unit structures	Structures of 10 or more units	Owner: Total	Lacking some or all plumbing facilities	Average number of rooms	Average value (dollars)	Per cent Negro	Renter: Total	Lacking some or all plumbing facilities	Average number of rooms	Average contract rent (dollars)	Per cent Negro	1.01 or more persons per room: Total	With all plumbing facilities	One person households	With female head of family	With roomers or boarders or lodgers
108	50	100	-	28	24	16		16		14		5.1	13000	100	2							1	2	-
109	79	100	-	41	14	25		23		20		5.5	15100	100	2					3	3	3	2	-
110	88	100	-	33	6	26		26		23		5.5	13700	100	2					3	3	2	2	-
111	34	100	-	27	15	15		15		14		5.1	13800	100								1	1	-
201	1086	99	-	26	3	258		256		234		6.1	18900	100	20		5.9	86	95	37	37	7	21	9
202	187	100	-	13	9	46		46		41		5.4	14000	100	4					6	6		4	
203	107	100	-	34	8	24	1	24		22	1	5.7	14400	100	2					2	2	2	1	
[illegible]	26	100	-	46	-	6		5		6					2					2	2			
205	52	100	-	60	8	10		10		10		4.9	12900	100						4	4	1	1	1
206	80	100	-	48	2	16		16		14		5.0	13200	100	2					4	4	2	2	
207	98	100	-	49	2	22		22		20		5.8	16900	100	2					4	4	1	2	1
208	17	100	-	29	-	6		6		6		5.0	13300	100	-					-	-	-	-	
209	134	94	-	45	2	33		33		33		6.0	19700	94						2	2	1	4	
210	212	98	-	49	3	58		58		53		6.0	22400	100	5		5.2		100	11	11	2	3	
211	136	100	-	53	1	34		34		31		5.3	16100	100	2					10	10		2	
212	261	100		50		61		61		54		5.8	16100	100	7		5.3	114	100	17	11	1	3	
105	[illegible]	16		37	4	2569	11	1763	106	1345	6	6.2	21200	6	932	5	4.4	99	31	135	137	358	186	36
101	114			23	11	40		28	3	25		5.6	16200		14		3.7	82		1	1	2	3	
103	58			28	5	21		21		9		5.4	14400		11		5.0	98				1	1	
104	81			44	7	23		23		18		5.8	17700		4					2	2		5	
105	8			25		3																		
106	33			33	6	26		26		20		5.2	18200		4							2	1	2
107	467	2		34	9	272		122		84		5.2	15800		70		4.2	69	2	4	4	19	20	
108	292	22		38	1	139	1	44	3						97	1	4.1	72	21	11	11	2	9	1
109	30	20		30	3	12		6	3						12		4.1	66	17			2		
110	317	26	1	39	3	144		78	1	13		5.9	21400		91		4.3	81	29	7	7	12	13	1
111	90	84		29	10	30		30		26		6.6	33300	85	3					1	1	1	2	1
112	56	7		32	7	15	1	15		14	1	6.1	21400	7	1					2	2	3	1	
113	1300	56		37	1	439	1	116	69	30		6.3	19700	31	397	1	4.2	108	55	42	40	28	55	22
201	97			35	3	32		15		22		5.1	17600		9		4.9	111		1	1	2	2	
202	154	5		37	5	44		44		40		6.4	26800	5	2					1	1	1	3	
203	84			31	6	28		28		28		7.2	26400									3	3	
204	97			38	4	25		25		22		7.2	29900		1					1	1	1	2	
205	62			31	7	18		18		17		7.4	28100		1									
206	42			39		12		12		11		7.5	27300		1									
207	573	1		41	3	164	1	164		151	1	6.5	22400	1	9		5.6	132		4	4	4	12	1
208	15			40	2	12		12		9		5.9	18700		3									
209	89	6		16	6	26		26		25		5.8	18900	4	1					2	2	4	1	
210	39			39	5	24		24		21		5.7	18900		3					2	2	3	1	
212	85			37	4	22		22		20		6.8	30100		2					1	1	1	1	1
213	144			35	3	42		42		39		7.0	29900		2							1		
214	119			29	8	37		37		35		7.3	31400		2							2	3	
215	65			32	3	19		19		19		6.9	27600									1	1	
216	261			42	2	74		74		69		7.4	30400		6		3	174					8	
217	47			19	17	19		19		14		5.6	17100		2							1	1	
219	5	100		20	20	2																		
227	15			20	7	6		6		5		6.2	18800		1							1		
229	33			33	6	9		9		9		5.6	14900											
230	57			35	11	15		15		13		6.2	17800		2							2		
231	46			39	3	15		15		14		5.5	17300		1					1	1			
232	61			39	7	17		17		17		5.7	19400							3	3			
233	104			30	9	33		33		26		5.6	16800		2		4.2	123		1	1			
234	401	3		37	5	119	3	115		106	2	5.8	19100	2	12	1	4.9	116		9	9	1	2	
301	25			28	4	7		7		6		5.3	17300		1					1	1	9	8	
302	557	5		34	3	187		114	28	86		5.2	18400	6	93		4.4	131	1	8	8	1		
303	195	10		42	1	59		59		56		5.8	20700	11						3	3	13	9	2
304	53			38	9	16		16		12		6.3	19200		4					2	2	1	3	1
305	89			37	5	22		22		21		6.6	19800		1					1	1			
306	162	3		41	3	42		42		39		6.0	17300	3	1								3	
307	246			39	7	72		70		65		5.8	17900		2		4.6	86		4	4	3	5	1
308	19			5	26	8		8		5		6.8			3									1
312	130			43	3	33		27							13		4.2	48		11	11	1	5	1
328	117	3		42	2	28		28		28		5.8	18000	4						3	3	1		
329	83			45		20		20		20		6.6	18900											
403	14			50	7	3																		
415	26	96		15	8	12	1	4	1	5		5.6		80	7	1	7.3	86	100			4	1	1
419	4					1																		
420	135	84		33	12	41	3	17		17	2	5.6	10800	89	12	1	4.8	53	75	2	6	9	3	
106	4832	58	2	36	13	1701	208	1230	74	771	69	5.2	12400	90	830	110	4.3	64	83	185	162	321	282	104
101	231	86		42	4	75	6	31		8	1	4.8	14700	100	67	1	4.2	98	68	14	14	8	20	
102	144	100		39	4	53	1	21	7	3					47		4.2	55	100	8	8	10	8	4
103	155	100		41	7	61		17		4					55		4.4	46	100	5	5	13	12	1
104	34	100		24	12	10		10		10		5.6	16000	100						1	1	3		
105	55	100		44	11	14		14		11		5.4	13900	100	3					3	3		4	1
106	24	100		29	17	8		8		8		5.6	20000	100						1	1	1	1	
107	18	100		39		5		5		5		5.2	13100	100						1	1	1	1	1
108	52	100		56		13		13		4					4		4.1	79	100	4	4	1	2	1
109	40	98		48	3	11		11		10		5.2	16400	100	1					1	1	1	3	
110	44	100		27	11	15		15		12		5.4	13000	100	2									
111	43	98		34	21	18	1	15		10		5.5	13100	100	2	1	4.4	59	100	1	1		4	
112	115	98	12	50	10	25	1	24		18	1	5.4	15100	100	2		4.9	85	100					
113	44	100	18	36	23	9		9		9		5.8	24100	100						6	6	2	4	2
115	32	100		44	6	9	1	9		4					5	1	4.0	59	100	1	1		1	2
116	30	100		43	10	8		7		5		5.4	16500	100	2					2	2			
117	109	100		51	7	26	2	26		11		5.4	11500	100	12	2	4.9	74	100	9	8	2	5	2
118	84	100		37	17	28	2	23		20	1	5.6	10400	100	8	1	4.5	56	100	2	1	8	2	3
119	20	100			30	11	1	8		6	1	5.2	13300	100	3							2		1

Figure 2.3 Tabular Census Data

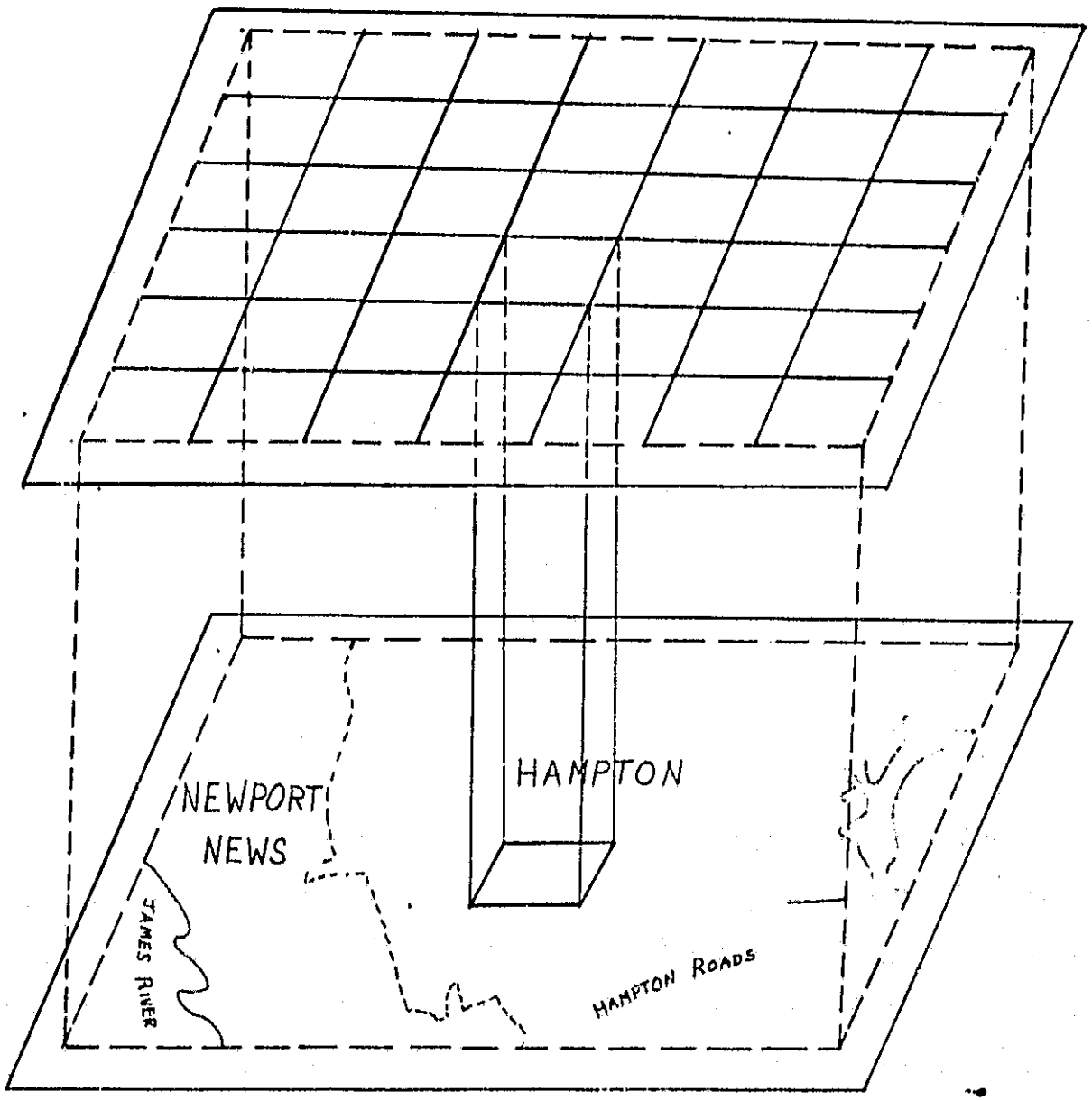

Figure 2.4 Illustration of the Overlay Technique for Determining Population Within One Square Mile

This means that approximately 40,000 numbers had to be processed to obtain the population model for a single terminal area. Figure 2.5 shows the finished product for one region of the Newport News-Hampton area.

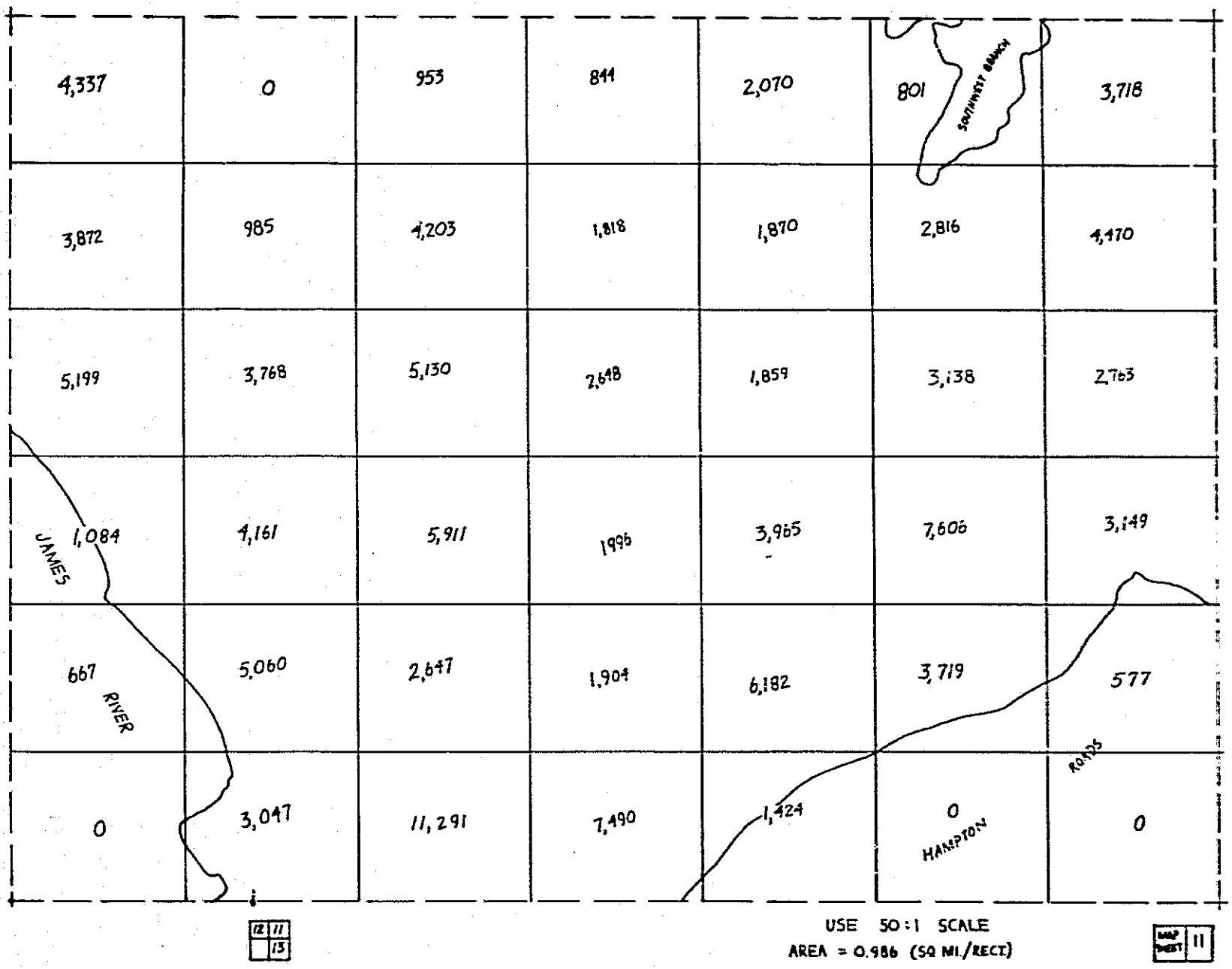

Figure 2.5 Compiled Population Data for Region II of the Newport News-Hampton Area

III. INTEGRATION OF POPULATION MODEL AND NOISE MODEL

A. Introduction

The subroutine called "Noise" computes the coordinates of the contour of the noise footprint given the attitude, altitude and thrust level of the aircraft. A typical footprint superimposed on the population model is shown in Figure 3.1. For the population blocks which are completely enclosed within the footprint, it a simple matter to determine the number of persons affected by 70 db. or more of noise. However, for the population blocks which lie partially inside and partially outside the footprint contour, the problem is more complex. And when one considers the fact that this calculation will be performed once every second during the forward integration of an approach trajectory and 21 times every second during the backward integration of the adjoint vectors required for the trajectory optimization, the need for efficiency is appreciated. Actually, it was originally planned to calculate the noise at every integration step or each .1 second. However, the continuity of the population distribution and the relatively low speed of the aircraft have permitted the less frequent calculations.

B. Time Saving Approximations

The subroutine for calculating the number of people inside the contour begins by selecting the equations for one quadrant of the noise contour and varying y in increments of 500 feet. This continues until a point of intersection of the noise surface with the ground is found. Suppose point 1 in Figure 3.1 is this first point. The procedure checks to see which population block this point is in. The x coordinates of the population boundaries intersecting the line joining the two noise contour points are determined and stored. The sub-area within each population block is then taken to be 100 feet times the lengths of the path just calculated. These areas are then weighted with the respective population densities. Next, y is incremented by 100 feet, point 2 is determined, and the procedure is repeated.

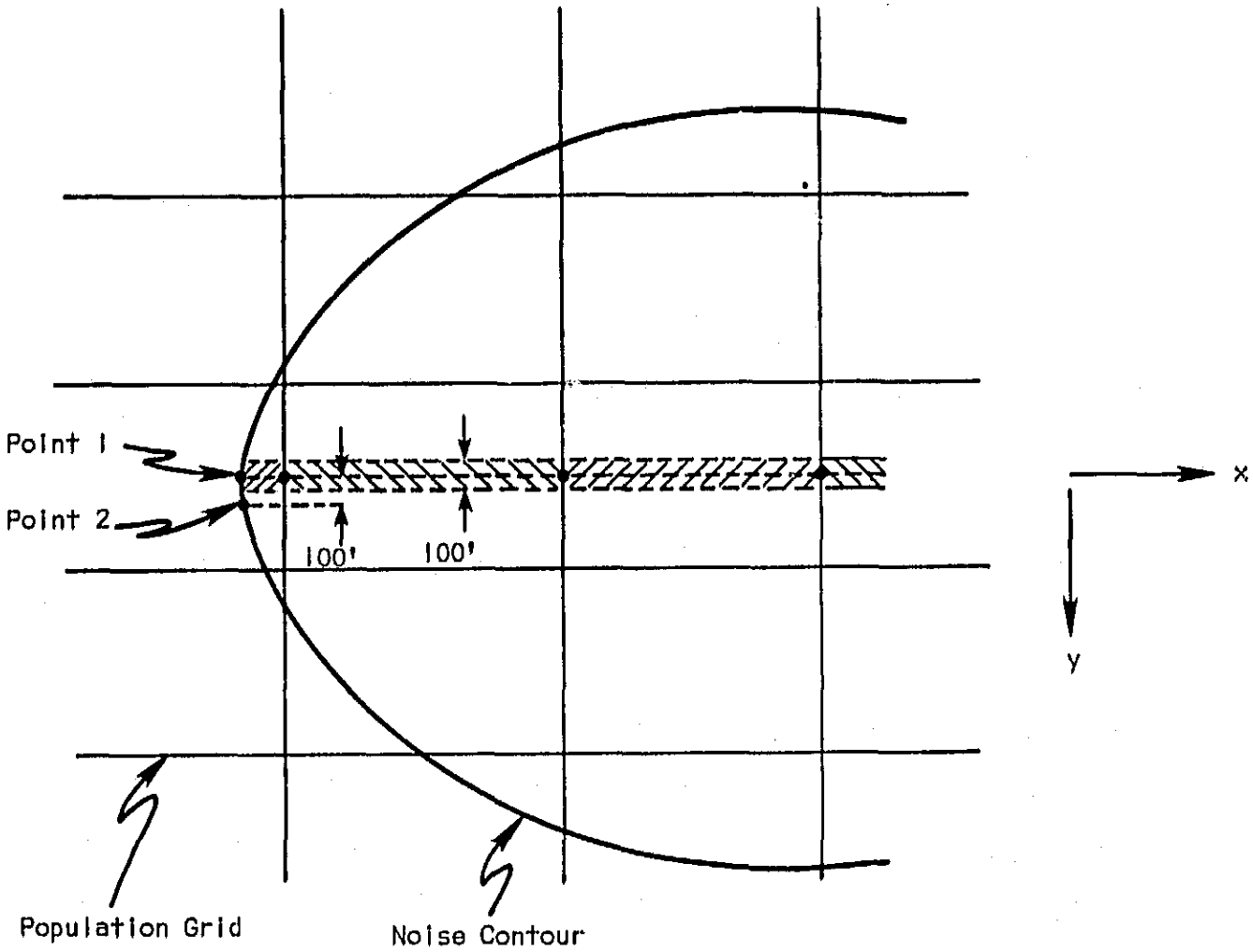

Figure 3.1 A Typical Noise Footprint Superimposed on the Population Grid

When the intersection of this quadrant of the noise model is completed, the next quadrant is considered. Previously all four quadrants had to be considered; however, a simple test was introduced based on the altitude, thrust level, roll angle and pitch angle of the aircraft. If this test is failed, then the two upper quadrants of the noise model need not be considered. This simplification along with the approximation of the area strips as rectangles, rather then trapezoids or triangles, has reduced the computation time required to one third of its original value. The average time presently required to determine the number of persons inside a noise footprint is 28 milliseconds.

C. Ground Track

Besides knowing the number of people affected by the noise and integrating this with respect to time, it is also desirable to have a graph of the ground track of this footprint. This envelope is obtained by determining the outer extremes of the footprint at every point in time and then passing lines through these points. The information obtained thusly is important in giving interpretation to the optimal trajectories.

IV. PROGRAMMING THE STEEPEST DESCENT OPTIMIZATION PROCEDURE

A. Outline of Steepest Descent

The method of steepest descent was first applied to optimal control problems by Bryson and Denham [2]. For the convenience of the reader and to clarify the notation to be used the main results are presented here.

The equations of motion along with a differential equation for the performance index are written in state variable form

$$\dot{X} = f(X,U) \tag{4.1}$$

The last component of X evaluated at final time is the performance index. Said differently, after one has chosen a performance index

$$\phi(X(T_f)) = \int_0^{T_f} L(X,U)dt, \tag{4.2}$$

then let

$$\dot{X}_{n+1} = f_{n+1}(X,U) = L(X,U) \tag{4.3}$$

with

$$X_{n+1}(0) = 0 .$$

The remaining components of the state vector differential equation are the description of the system to be controlled which in our case is the aircraft. If these equations are of order n, then equation (4.1) will be of order n + 1. It is important to realize that $\dot{X}_1$ through $\dot{X}_n$ do not depend on X_{n+1} although X_{n+1} may depend on X_1 through X_n as well as U.

Along with the performance index there may be boundary conditions which must be satisfied at t_f. These boundary conditions are written as the scalar equation

$$\psi(X(t_f)) = 0 \ . \tag{4.4}$$

Also if t_f is not prespecified one must formulate a stopping condition to establish t_f. This takes the form of the scalar equation

$$\Omega(X(t_f)) = 0 \tag{4.5}$$

An initial estimate of the control history is made and equations (4.1) are integrated forward in time until the stopping condition (4.5) is satisfied. Then an iterative procedure is used to successively drive $\psi(X(t_f))$ toward zero and simultaneously minimize $\phi(X(t_f))$.

The iterative procedure requires the backward integration of the following n x 1 vector differential equations

$$\dot{\lambda}_\phi = - \left(\frac{\partial f}{\partial x}\right)^T \lambda\phi \tag{4.6a}$$

$$\dot{\lambda}_\psi = - \left(\frac{\partial f}{\partial x}\right)^T \lambda\psi \tag{4.6b}$$

and

$$\dot{\lambda}_\Omega = - \left(\frac{\partial f}{\partial x}\right)^T \lambda\Omega \tag{4.6c}$$

with boundary conditions

$$\lambda_\phi(t_f) = [\partial\phi(x(t_f))/\partial x(t_f)]^T \tag{4.7a}$$

$$\lambda_\psi(t_f) = [\partial\psi(x(t_f))/\partial x(t_f)]^T \tag{4.7b}$$

and

$$\lambda_{\Omega}(t_f) = [\partial\Omega(x(t_f))/\partial x(t_f)]^T . \tag{4.7c}$$

The control for the next iteration is given by the m x 1 vector equation

$$U_{new} = U_{old} - W^{-1}(\gamma_{\phi}^T - \gamma_{\Omega}^T I\psi\phi/I\psi\psi)\left[\frac{dP^2 - d\psi^T d\psi/I\psi\psi}{I\phi\phi - \psi\phi^2/I\psi\psi}\right]^{1/2} + W^{-1}\gamma_{\psi}^T d\psi/I\psi\psi \tag{4.8}$$

where the m x 1 vector

$$\gamma_{\phi} = [\gamma_{\phi}^T - \gamma_{\Omega}^T (t_f)/\dot{\Omega}(t_f)]\partial f/\partial u, \tag{4.9a}$$

the m x 1 vector

$$\gamma_{\psi} = [\gamma_{\psi}^T - \gamma_{\Omega}^T \dot{\psi}(t_f)/\dot{\Omega}(t_f)]\partial f/\partial u, \tag{4.9b}$$

the scalar

$$I_{\psi\psi} = \int_0^{t_f} \gamma_{\psi}^T W^{-1}\gamma_{\psi} dt, \tag{4.10a}$$

the scalar

$$I_{\psi\phi} = \int_0^{t_f} \gamma_{\psi}^T W^{-1}\gamma_{\phi} dt, \tag{4.10b}$$

and the scalar

$$I_{\phi\phi} = \int_0^{t_f} \gamma_{\phi}^T W^{-1}\gamma_{\phi} dt. \tag{4.10c}$$

The change in control during an iteration is limited by selecting the scalar

$$dP^2 = \int_0^{t_f} \delta U^T W \delta U dt. \qquad (4.11)$$

This constraint when properly used ensures that linearizations upon which the iterative procedure is based will be valid. The scalar quantity $d\psi$ is the amount of reduction in $\psi(x(t_f))$ which one seeks during a particular iteration. If the radical of (4.8) is negative then one has asked for too much reduction in ψ for the change in control permitted by (4.11) and $d\psi$ must be reduced until the radical is positive. Within the accuracy of the linearization the control given by equation (4.8) will then yield the change in ψ specified and use the remaining freedom allowed by equation (4.11) to reduce ϕ.

B. Partial Derivative Calculation

The calculation of the n x n partial derivatives $\partial f/\partial x$ and the n x m partial derivatives $\partial f/\partial u$ required in equation (4.6) and (4.9) may be accomplished analytically or numerically. If accomplished analytically it still requires evaluation of the n^2 elements of $\partial f/\partial x$ and the n x m elements of $\partial f/\partial u$ at every point in time. This is seen from the following

$$\partial f/\partial x = \begin{bmatrix} \partial f_1/\partial x_1, & \partial f_1/\partial x_2, & \cdots & \partial f_1/\partial x_n \\ \vdots & & & \vdots \\ \partial f_n/\partial x_1, & \partial f_n/\partial x_2, & \cdots & \partial f_n/\partial x_n \end{bmatrix}_{X,U} \qquad (4.12a)$$

and

$$\partial f/\partial u = \begin{bmatrix} \partial f_1/\partial u_1, & \partial f_1/\partial u_2, & \ldots & \partial f_1/\partial u_m \\ \vdots & & & \\ \partial f_n/\partial u_1, & \partial f_n/\partial u_2, & \ldots & \partial f_n/\partial u_m \end{bmatrix}_{X,U} \qquad (4.12b)$$

If accomplished numerically, by finite differences, $n + (n \times n) + (n \times m)$ evaluations are required. This is seen from the following

$$\frac{\partial f_i}{\partial X_j} \simeq \frac{f_i(X_1, X_2, \ldots, X_j + \Delta X_j, \ldots X_n, U) - f_i(X_1, X_2, \ldots, X_j \ldots X_n, U)}{\Delta X_j} \qquad (4.13a)$$

and

$$\frac{\partial f_\ell}{\partial U_k} \simeq \frac{f_\ell(X, U_1 \ldots, U_k + \Delta U_k \ldots U_m) - f_\ell(X, U_1, \ldots, U_k, \ldots, U_m)}{\Delta U_k}$$

The number of calculations for the two methods is almost equal. Furthermore non-analytical data such as that from wind tunnel can be used much more conveniently via the second method. Also opportunities for programming errors are fewer if the second method is used. For these reasons the partial derivatives are determined numerically.

C. Memory Storage Requirements

It is seen from equations (4.6), (4.8) and (4.9) that the values of X and U must be stored at every point in time during the forward integration. If U is m x 1, X is n x 1 and the time quantization is chosen as Δt, this storage requires $(n + m)t_f/\Delta t$ locations. Also from (4.8) and (4.9) it is seen that γ_ϕ and γ_Ω must be stored at every point in time during the backward integration. This storage requires $2mt_f/\Delta t$ locations.

It is important to note that this Δt referred to as the time quantization is not necessarily the time step for the numerical integration. Rather it represents the time between changes in the control function. As was pointed out in Section III a time step of .1 seconds was selected for the numerical integration. However if this value is used for the time quantization a run of 300 seconds with n = 13 and m = 9, would require $(n + 3m)t_f/\Delta t$ = 120,000 storage locations.

To reduce this number to a more tolerable value it was decided to use a Δt of 1 second. This brings the storage requirements to 12,000 and still allows a reasonably fast changing control. Experiments were performed to confirm that $\partial f/\partial x$ and $\partial f/\partial u$ do not vary excessively during a one second interval. In fact some elements need be updated only every ten seconds.

D. Numerical Integration Method

Initially, the fourth-order Runge-Kutta method was used for numerical integration of the differential equations describing the aircraft. This method was used because it is self-starting, generally reliable and was familiar to the authors. However, because of the high order of the system and the amount of computation time required by the fourth-order Runge-Kutta procedure, other methods were considered. One method which appeared attractive was the Milne-Reynolds predictor-corrector technique [3]. This method requires values of the dependent variables for four previous points in time and cannot be used for start-up; however, it can be used after a method such as the Runge-Kutta has been used for a few samples. The advantage of the Milne-Reynolds method is that it requires only two evaluations of the right hand side of the differential equations per integration step whereas the fourth-order Runge-Kutta method requires four evaluations. With our differential equations being nonlinear and requiring table look-up of wind tunnel data, this evaluation is the most time consuming part of the numerical integration.

The Milne-Reynolds method proved very accurate with deviations from the Runge-Kutta simulation occurring only after the fourth significant

figure. The computation time was reduced from 1.07 seconds per second of simulated time to .61 seconds per second of simulated time. This procedure is the one presently being implemented in our simulation of the aircraft.

Some experimentation on step size was performed. It was determined that .1 seconds was the largest step which could be used by either integration method and still yield accurate results.

E. Choice of Backward Integration Method

For the nonlinear system under consideration (equation (4.1)) it was determined that the maximum integration step size which yielded accurate results was .1 seconds. Assuming that this would also hold for the incremental model and realizing the eigenvalues of $(\partial f/\partial x)^T$ are the same as those of $\partial f/\partial x$ tells us that the maximum step size for equations (4.6) using the Milne-Reynolds methods would also be .1 seconds. This means that 10 integration steps would be required between storage points. The Milne-Reynolds method requires two evaluations of the right hand side of the differential equations for each integration step. This would be 20 evaluations for one second. Each evaluation requires the multiplication of the n x n matrix $(\partial f/\partial x)^T$ by the n x 1 vector or n^2 multiplications. Doing this 20 times per Δt and once for each of the three λ vectors yields 60 n^2 multiplications per 1 second of simulated time.

Referring to equations (4.6) and (4.7) it is noted that the three vector differential equations are identical except for their boundary conditions. This suggests the possibility of effectively using the transition matrix as an alternate means of obtaining the solutions of these equations, i.e.

$$\lambda(t - \Delta t) = e^{-(\partial f/\partial x)^T(-\Delta t)}\lambda(t) \tag{4.14}$$

Using a Padé approximation [4] to the matrix exponential one has

$$e^{(\partial f/\partial x)^T\Delta t} \approx (I - \frac{1}{2}A + \frac{1}{10}A^2 - \frac{1}{120}A^3)^{-1}(I + \frac{1}{2}A + \frac{1}{10}A^2 + \frac{1}{120}A^3) \tag{4.15}$$

where

$$A = (\partial f/\partial x)^T \Delta t$$

The Padé approximation of (4.15) has one percent accuracy [4] up to $\lambda_{max}\Delta t = 2.8$. The maximum eigenvalue of $\partial f/\partial x$ was estimated to be 2 which implies that equation 4.15 will be accurate for $\Delta t \leq 1.4$ seconds and therefore will be satisfactory for the required Δt of one second. The number of multiplications required to compute equation (4.15) is $4n^3$. To multiply the transition matrix by each of the three λ(adjoint) vectors requires an additional $3n^2$ multiplications.

Thus to integrate the three adjoint vecotrs, equation (4.6), backward one second requires $4n^3 + 3n^2$ multiplications plus the calculation of $\partial f/\partial x$. This is to be compared with the $60n^2$ multiplications plus the calculation of $\partial f/\partial x$ required using the Milne-Reynolds method. For $n = 12$ these numbers become 7,344 and 8,640 multiplications. Assuming a computation time of 10 μsec per multiplication this is a difference of .01296 seconds of computation per second of integration. When compared to the time required for the determination of $\partial f/\partial x$ which is .364 seconds this difference is seen to be quite small. It was therefore decided to use the most convenient method for the integration. This turned out to be the Milne-Reynolds method since it had already been programmed for the forward integration.

F. Reduction of System Order

Because of the extreme complexity of this problem, every effort has been made to do things as efficiently as possible. This has taken the form of simplifying approximations in some cases, proper choice of integration methods, minimization of memory storage requirements, etc. An additional simplification has involved the differential equation describing the time rate change of the weight of the aircraft. Because of the relatively short flight time under consideration, (<500 seconds) the percentage change in weight is less than 1%. It was thus decided to

examine the effect of neglecting this equation. On a simulation of 300 seconds using the same open loop control for both cases, with and without the weight change equation, the final altitudes differed by only 10 feet out of a total change of 2000 feet. Also the flight path angles differed by only .06 degrees out of 3 degrees. It was then decided that the weight change equation could be neglected without appreciably affecting the aircraft behavior. This reduced the dimension of the state vector from thirteen to twelve.

Another simplifying assumption was to maintain the landing-gear down through the approach maneuver. Previously the landing-gear position, up or down, had been treated as a control variable. However, the effect of the landing gear position on lift and drag was found to be small compared with the effects of the main control surfaces. Therefore, to reduce the complexity of the optimization procedure it was decided to have the landing-gear lowered at a specified range from the runway. This simplification reduced the dimension of the control vector from nine to eight. The states and controls are defined as: x_1 - velocity, x_2 - angle of attack, x_3 - side slip angle, x_4 - roll rate, x_5 - pitch rate, x_6 - yaw rate, x_7 - yaw angle, x_8 - pitch angle, x_9 - roll angle, x_{10} - ground coordinate x, x_{11} - ground coordinate y, x_{12} - altitude, x_{13} - performance index, u_1 - thrust, u_2 - elevator, u_3 - flaps, u_4 - spoiler panels 2 and 3, u_5 - spoiler panels 6 and 7, u_6 - rudder, u_7 - aileron and u_8 - stabilizer. Controls u_2 and u_8 are assumed independent.

G. Selection of Stopping Condition

For an optimization problem with unspecified final time one must have a way of determining t_f. Since there may be several terminal constraints such as those on attitude, velocity, altitude, etc., the chances are slim that all of these conditions will be satisfied simultaneously, especially during the first few iterations. The stopping condition must be a scalar quantity which is certain to be satisfied even for a very poor trajectory since the initial guess may indeed be a poor trajectory.

The choice for stopping condition for the aircraft landing problem was taken to be the time rate of change of distance between the aircraft and the runway. As long as this distance is being decreased, the problem continues to run; however, whenever the distance begins to increase, i.e. just as the rate change goes through zero, the problem is terminated. This stopping condition will work whether or not the aircraft passes directly over the runway and therefore can be used even though the initial trajectory may have a large final error.

The equation for the stopping condition is

$$\Omega(x(t_f)) = \frac{1}{2}\frac{d}{dt}\left[(x_{10} - x_{10_F})^2 + (x_{11} - x_{11_F})^2\right] \qquad (4.16a)$$

or

$$\Omega(x(t_f)) = (x_{10} - x_{10_F})f_{10} + (x_{11} - x_{11_F})f_{11} \qquad (4.16b)$$

where the subscripts F represent the specified final conditions.

H. Selection of Boundary Conditions and Coefficients

The steepest descent optimization procedure has a dual goal of not only minimizing the performance index but also satisfying the boundary conditions at final time. There are nine boundary conditions which must be met at final time. These could be specified as nine separate equations, but this would necessitate the use of nine λ_ψ vectors. As a means of minimizing the complexity of the problem it was decided to merge the nine boundary conditions into a single constraint equation which could be driven to zero if and only if all nine boundary conditions were met.

A quadratic form was chosen for the constraint equation with coefficients chosen so that "equal" errors would contribute equally to the ψ function, e.g. it was felt that a .1 degree error in flight path angle should contribute the same amount as a 100 foot error in position etc. The final form of the constraint equation follows:

$$\psi(x(t_f)) = .01(x_1 - x_{1_F})^2 + 400[(x_8 - x_2) - (x_{8_F} - x_{2_F})]^2$$
$$+ 7.5 \times 10^5(x_4 - x_{4_F})^2 + 1.5 \times 10^6(x_6 - x_{6_F})^2$$
$$+ 5 \times 10^4(x_7 - x_{7_F})^2 + 1.5 \times 10^4(x_9 - x_{9_F})^2 \qquad (4.15)$$
$$+ 2 \times 10^{-4}(x_{10} - x_{10_F})^2 + 2 \times 10^{-4}(x_{11} - x_{11_F})^2$$
$$+ 3 \times 10^{-3}(x_{12} - x_{12_F})^2$$

1. Selection of Performance Index

At the beginning of this project it was decided that noise to the population residing near the air terminal, passenger discomfort, fuel and time should all enter into the performance index. The noise model along with the population model yields the number of persons receiving noise in excess of 70 pndb. This quantity is integrated with respect to time and the cumulative quantity is called noise with dimensions of people-seconds.

The time is simply the duration of the flight. It is important to keep this time reasonably small in order to minimize the congestion among planes waiting to land. Fuel utilized during the descent maneuver is included for obvious economic reasons. Passenger comfort is important and must be considered lest the optimization procedure develop a trajectory with violent maneuvers. Constraints such as structural limitations of the aircraft are included within the aircraft model; however, one could operate within these constraints and still cause considerable discomfort to the average passenger. Thus a penalty function is included which contributes very heavily to the performance index whenever the comfort limits are exceeded.

In addition to these quantities, certain other penalty functions are added to ensure that the aircraft does not exceed its design capabilities. These include penalties for exceeding limits on altitude, altitude ascent rate, altitude descent rate, angle of attack, minimum velocity, etc.

The performance index including the penalty functions is given below.

$$\phi = x_{n+1}(t_f) \int_0^{t_f} f_{n+1}(X,U)dt \tag{4.16a}$$

$$f_{n+1} = 5 \times 10^{-3} \times \text{FUEL RATE} + 10^{-4} \times \text{NOISE RATE} + 7 \times 10^{-3}$$

$$+ \text{PENALTY FUNCTIONS} \tag{4.16b}$$

The coefficients above were selected so that time and fuel would contribute to the performance index approximately ten percent as much as noise. The number 7×10^{-3} is the coefficient for time. Note that the time rate, $d/dt(t)$, is one.

The penalty functions follow

$$\text{PENALTY FUNCTIONS} = \frac{A_{vert}^2}{(.1014)^2} + \frac{A_{trans}^2}{(.2047)^2} + \frac{A_{lat}^2}{(1.1667)^2} + \frac{A_{pitch}^2}{(5.8336)^2}$$

$$+ \frac{A_{well}^2}{(5.8336)^2} + \frac{A_{yaw}^2}{(.7778)^2} +$$

$$\left(\frac{f_{12}}{\text{Max Desc. Rate}}\right)^{100} + \left(\frac{f_{12}}{\text{Max Asc. Rate}}\right)^{100} + \left(\frac{x_{12}}{\text{Max Alt.}}\right)^{100}$$

$$+ \left(\frac{\text{Min. Alt.}}{x_2}\right)^{100} + \left(\frac{\text{Load Factor} - .75}{1.75}\right) + \left(\frac{x_2 - 10}{15}\right)^{100}$$

$$+ \left(\frac{x_2}{\text{Low Speed Buffet Coeff}}\right)^{100} + \left(\frac{C_L}{\text{High Speed Buffet Coeff}}\right)^{100}$$

$$+ \left(\frac{1.1\, V_{stall}}{x_1}\right)^{100}$$

The first group of terms represents the comfort index [1,5]. As long as this term is less than unity, the passengers are comfortable. The number raised to the one hundredth power is very small and contributes almost nothing to the performance index. When the accelerations are

large however and the bracketed term exceeds unity, then the performance index receives a large positive input. The f_{12} terms represent rate change of altitude. The first f_{12} term applies during descent using a maximum descent rate of 250 feet/sec. The second f_{12} term applies during ascent and uses a maximum ascent rate of 100 feet/sec. The x_{12} terms are used to keep the aircraft model within acceptable altitude limits. Without flaps, h_{max} is 35,000 feet. With flaps, h_{max} is 20,000 feet. The limit, h_{min}, is 100 ft. The load factor term reflects the structural limitations on the aircraft. The first term in x_2 is used to maintain the angle of attack between -5 and +25 degrees. The second term in x_2 keeps the angle of attack below that value which causes low speed buffet. The term in C_L keeps the lift coefficient below that value which causes high speed buffet. Logic in the program is used to switch in the appropriate terms depending on the state of the aircraft. The final term is used to penalize whenever the aircraft velocity gets near stall velocity. Each of these terms in the penalty function is raised to the power of 100 in an attempt to ensure that none of the limitations will be exceeded.

V. CONSTANT GLIDE-SLOPE APPROACHES

A. General Utility of Performance Measure

The selection of a performance measure to be associated with a task is generally non-trivial. It forces one to give serious thought to what the real objectives are and then to express those objectives in mathematical form. One normally formulates a performance index as a part of an optimization package; however, the use of a performance measure should not be restricted to variational procedures. Many times there may be several alternative sub-optimal strategies which one would like to compare. It may be that these strategies are easy to implement, acceptable to the users, or have other desirable characteristics. In situations such as these, a performance measure can be very useful as a means of evaluating the various strategies.

B. Three-Degree and Six-Degree Glide Slopes

Two approach trajectories of interest are the three-degree and the six-degree constant glide slope trajectories. It was decided to simulate these flights as a means of testing our aircraft simulation and also to compare the performance of the trajectories. The alignment and position of the Patrick Henry Airport runway are shown in Figures 5.3, 5.6, 5.9 and 5.12. The flights were begun at a range of 16 nautical miles from the end of the runway at the altitude obtained by extending the appropriate glide slope back from a point 383 feet high and 1.17 nautical miles out. This termination point allows a three-degree glide slope to be used for the last 1.17 nautical miles of the landing maneuver. Approaches were simulated for runways 6, 24, 2 and 20, each at the 3° and the 6°glide slopes, yielding eight trajectories. On our coordinate system, Figures 5.3, 5.6, 5.9 and 5.12, runway 6 is at an angle of -27°, runway 24 is at an angle of 153°, runway 2 is at an angle of -72° and runway 20 is at an angle of 108° measured with respect to the x axis.

The actual flight path angles are 2.79° and 5.85°. Additional adjustments on the open loop controls could have made these values closer

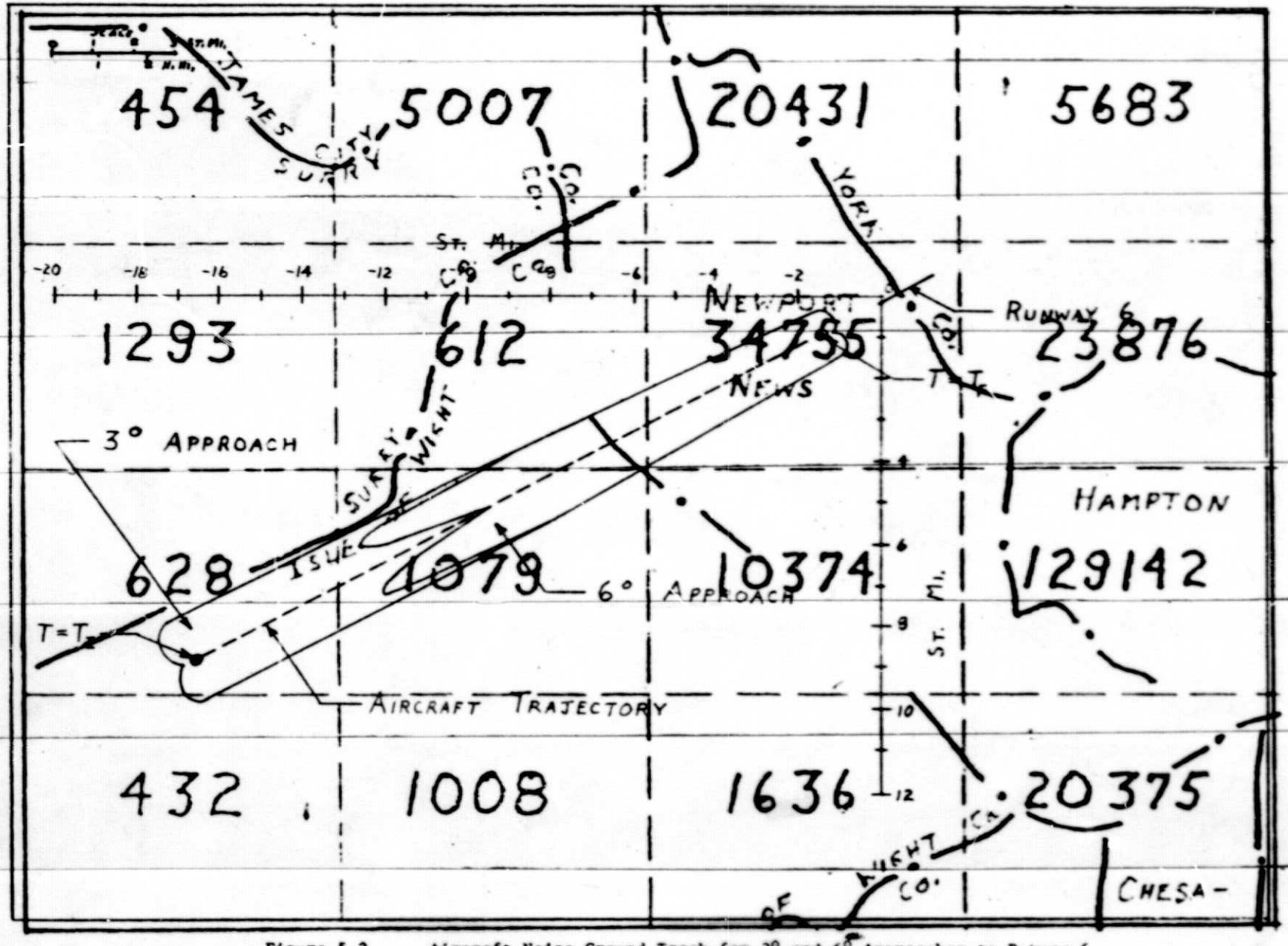

Figure 5.2 Aircraft Noise Ground Track for 3° and 6° Approaches to Runway 6.

Figure 5.1 Population Map of Terminal Area Surrounding Runway 6.

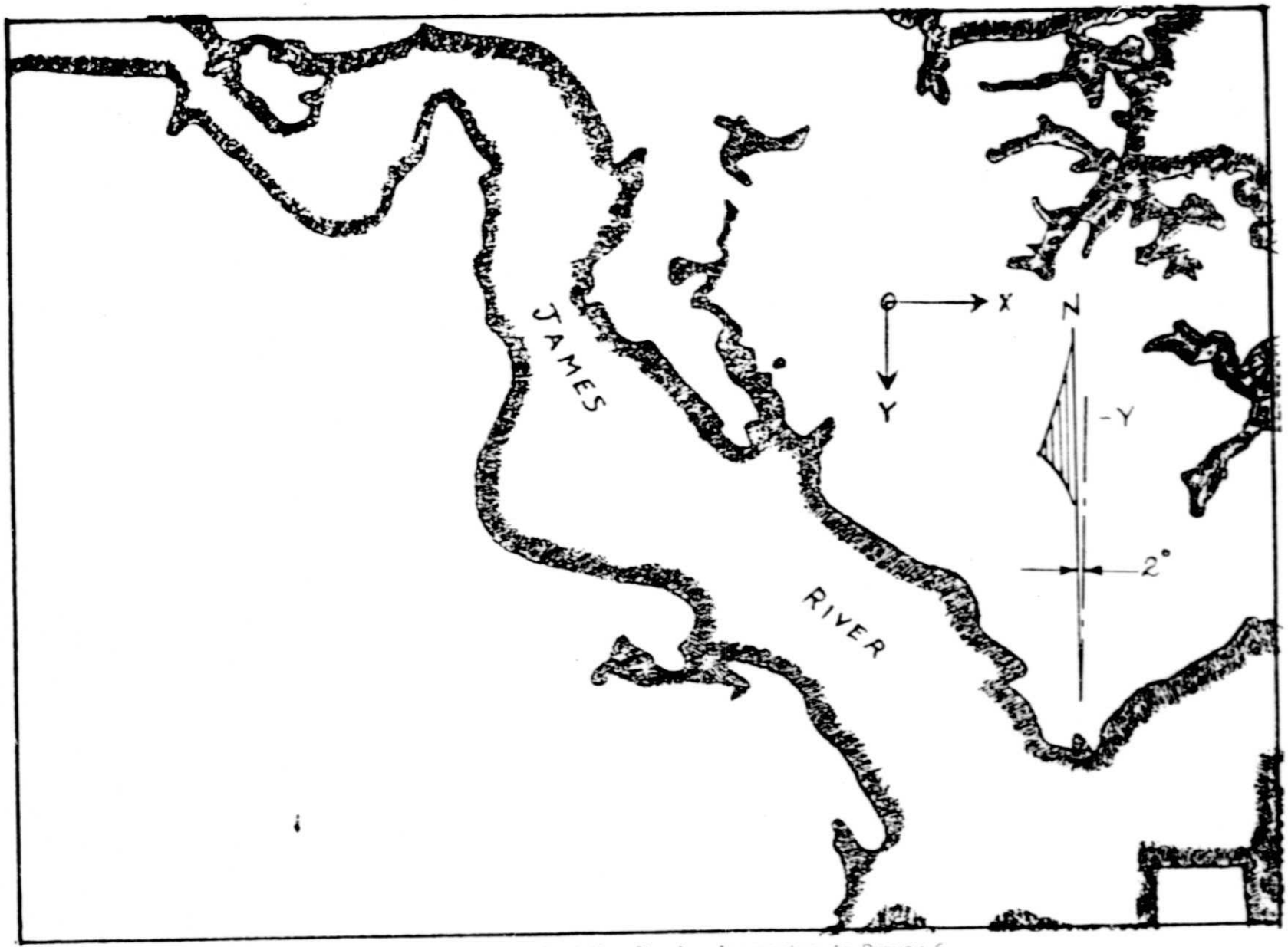

Figure 5.3 Topographical Map Showing Approaches to Runway 6

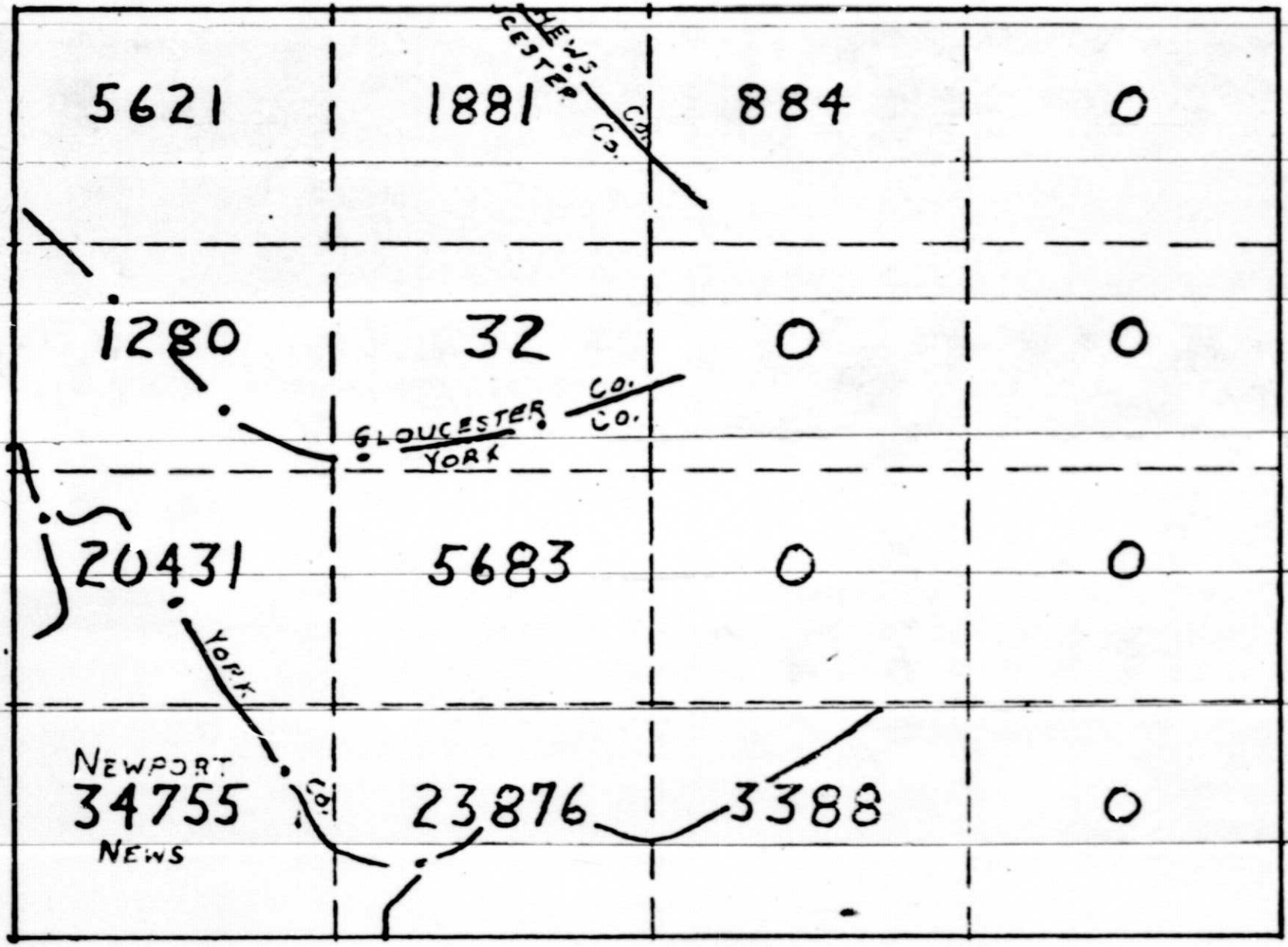

Figure 5.4 Population Map of Terminal Area Surrounding Runway 24.

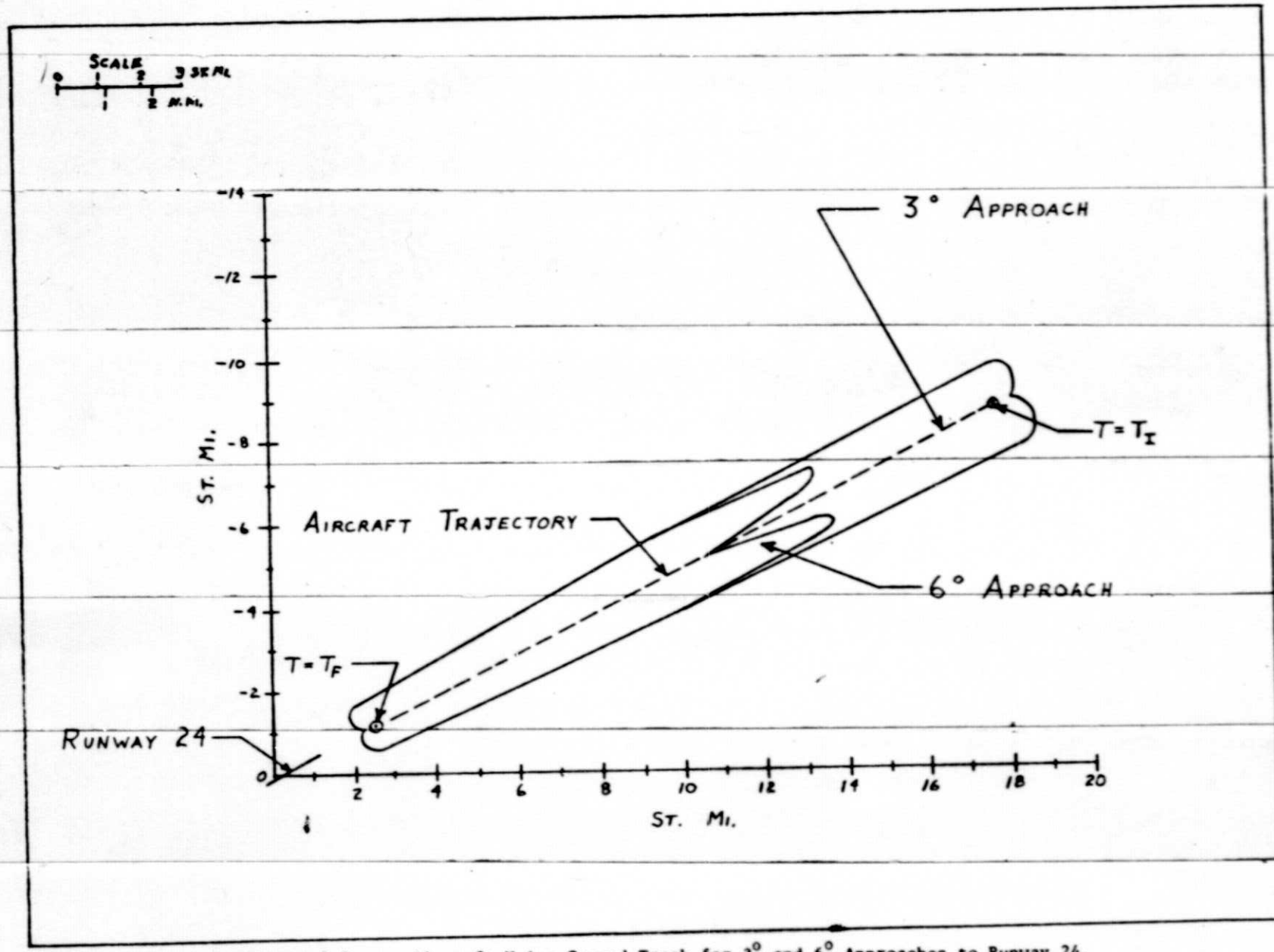

Figure 5.5 Aircraft Noise Ground Track for 3° and 6° Approaches to Runway 24.

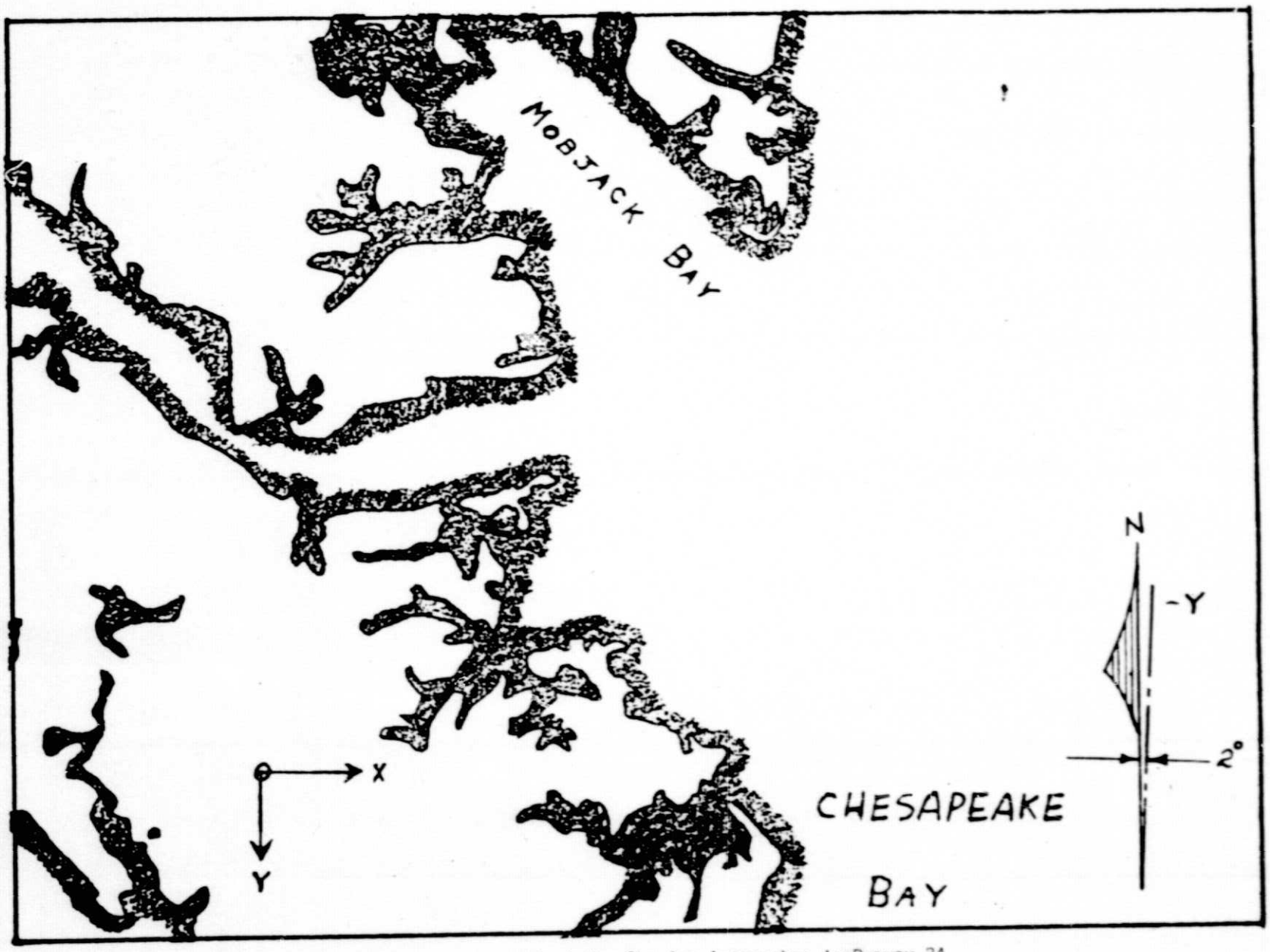

Figure 5.6 Topographical Map Showing Approaches to Runway 24

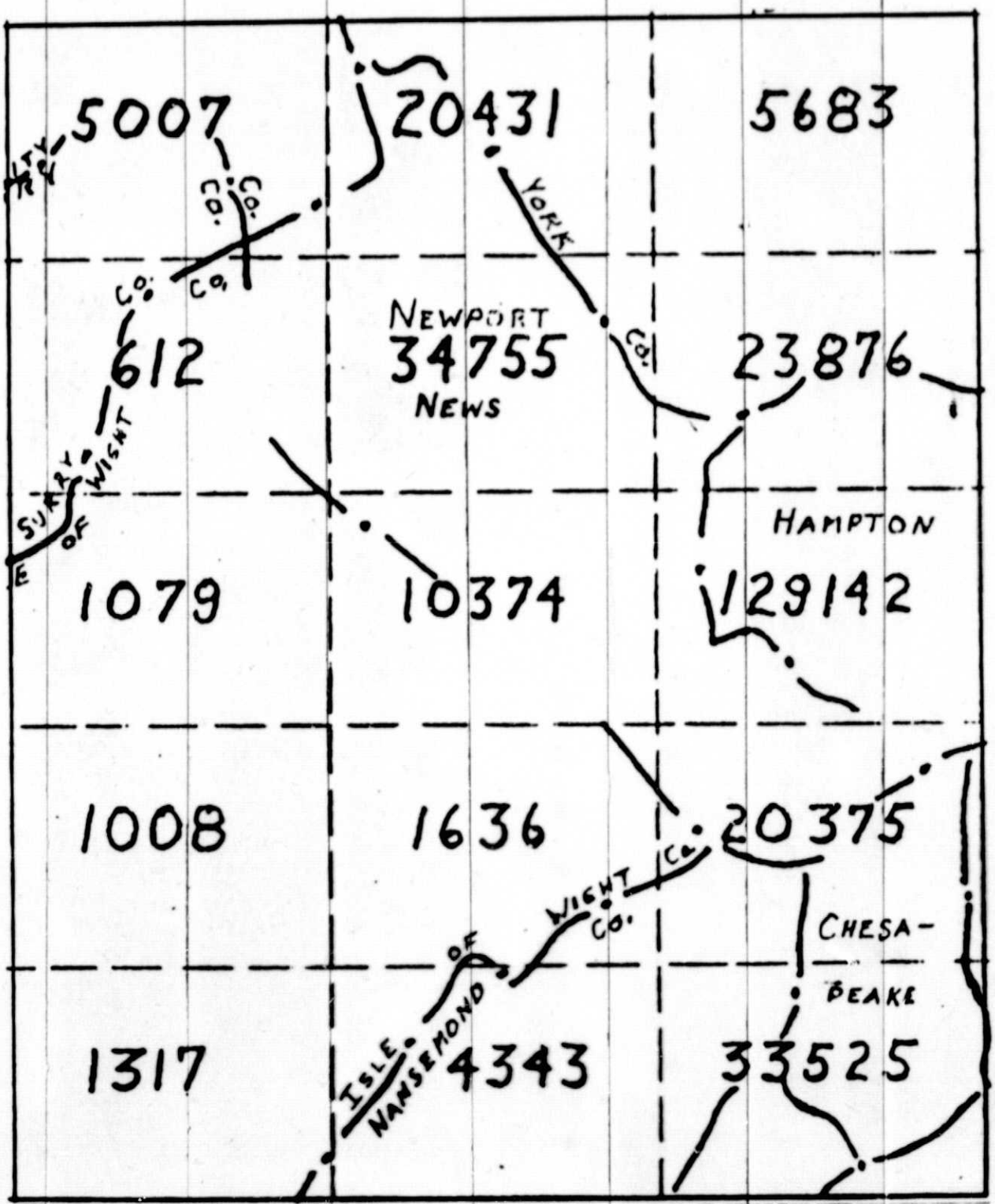

Figure 5.7 Population Map of Terminal Area Surrounding Runway 2.

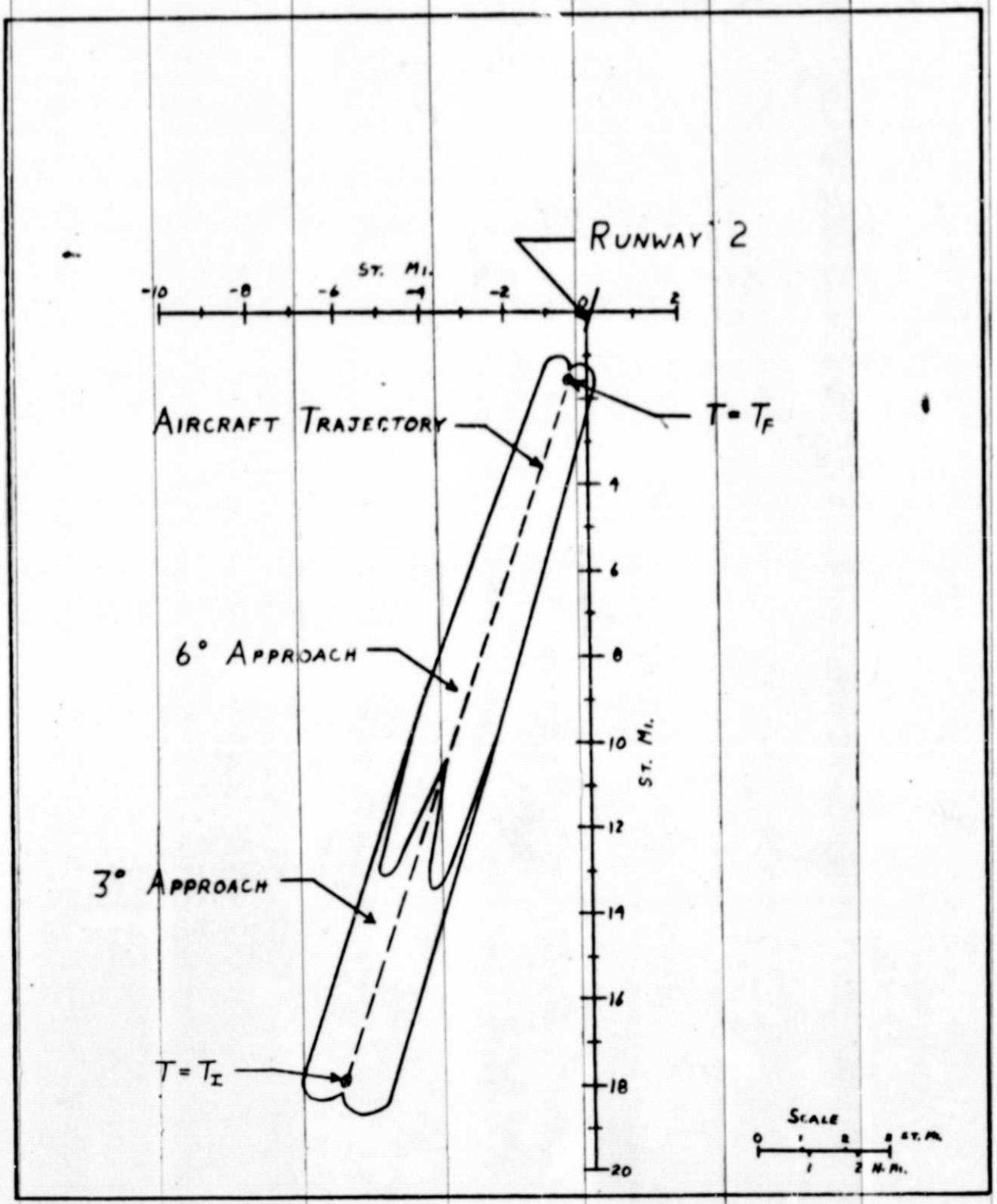

Figure 5.8 Aircraft Noise Ground Track for 3° and 6° Approaches to Runway 2.

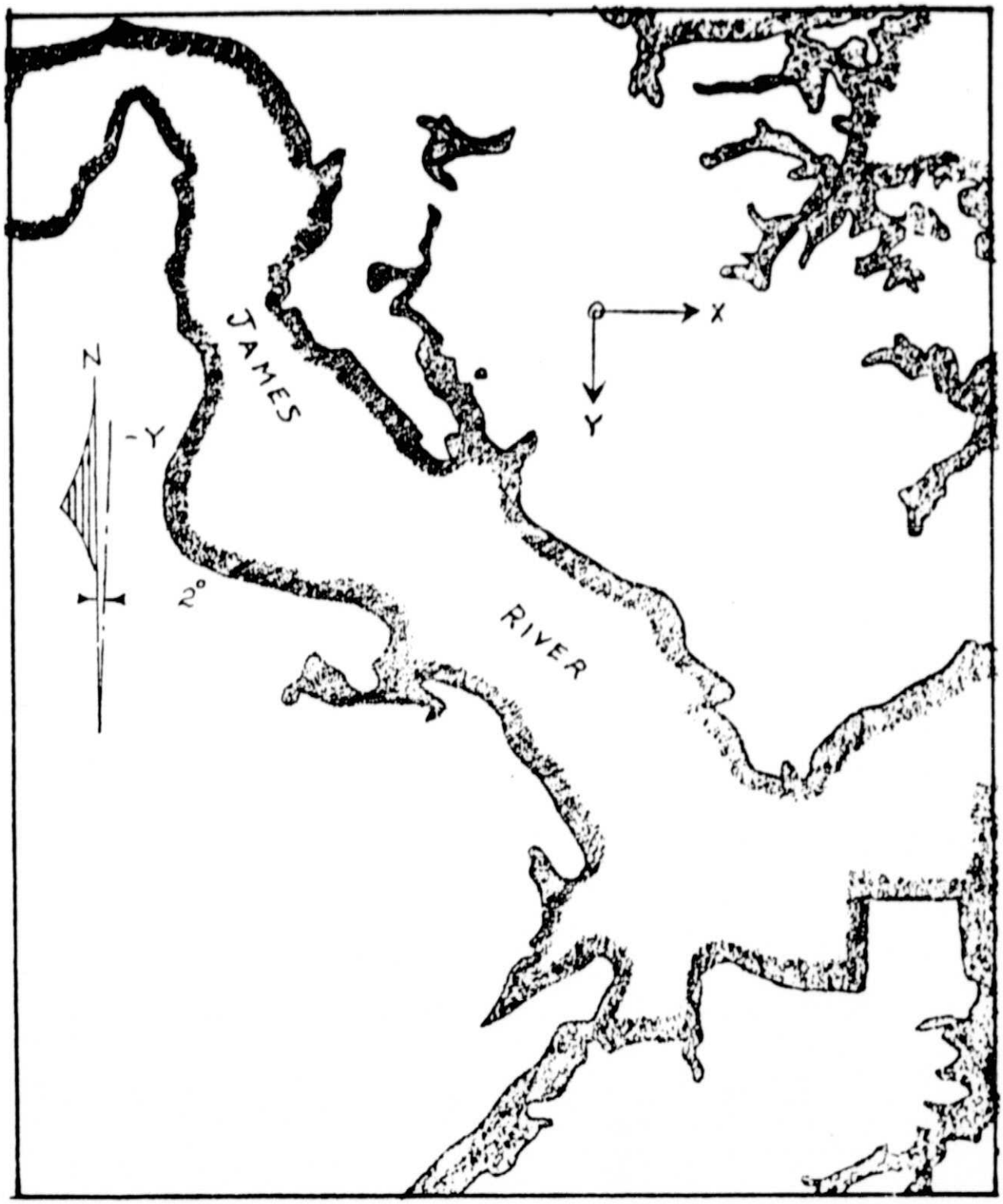

Figure 5.9 Topographical Map Showing Approaches to Runway 2.

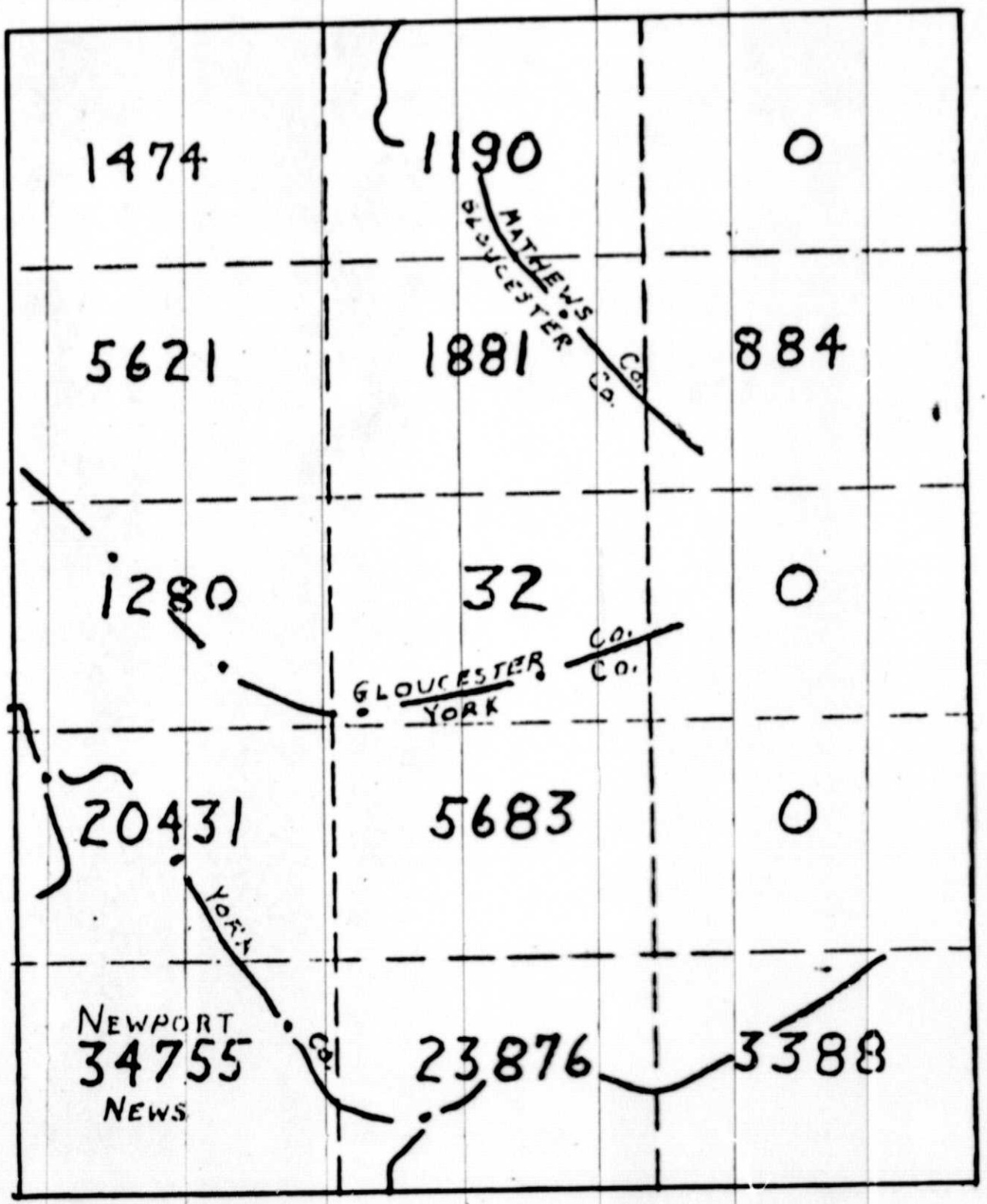

Figure 5.10 Population Map of Terminal Area Surrounding Runway 20.

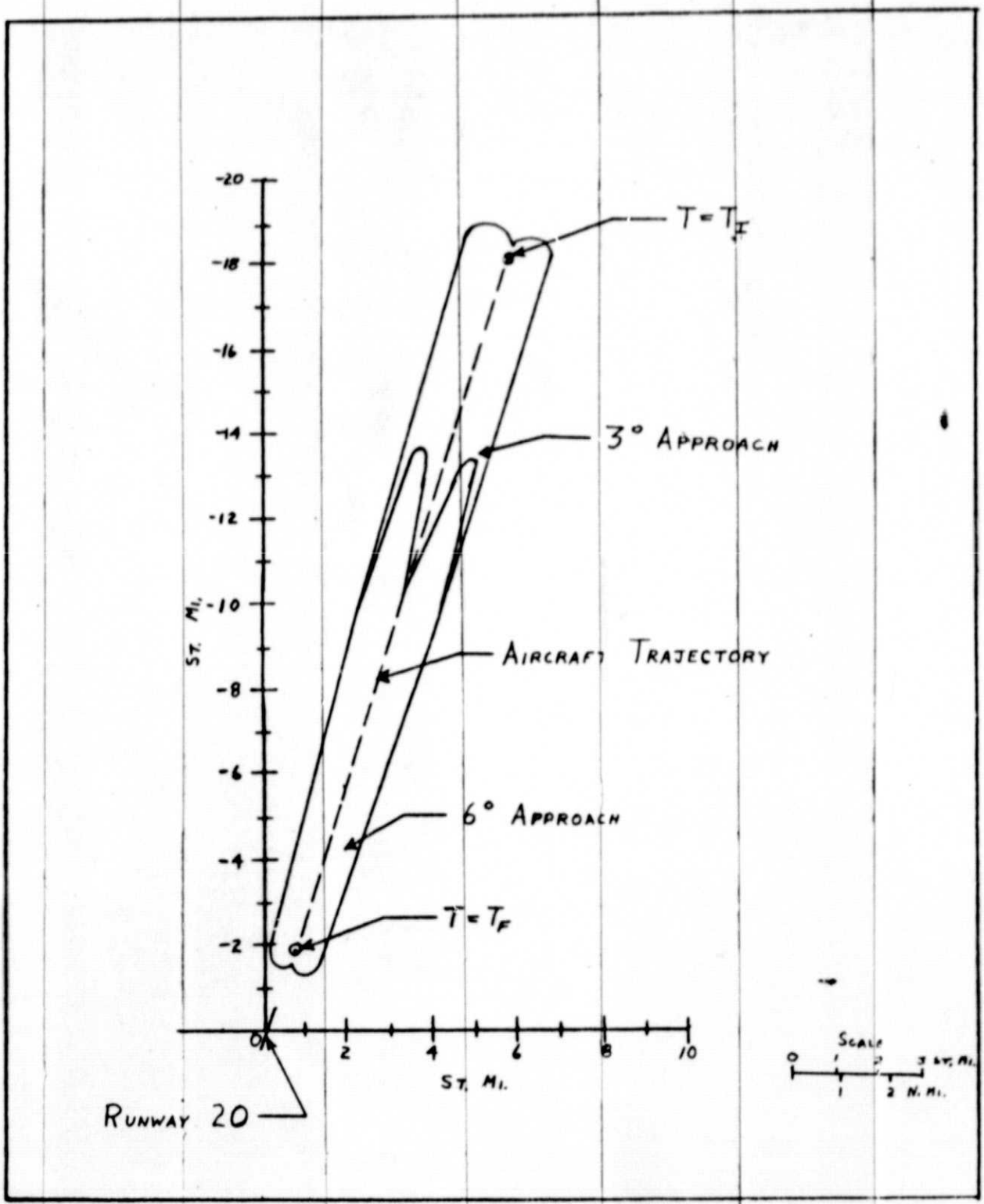

Figure 5.11 Aircraft Noise Ground Track for 3° and 6° Approaches to Runway 20.

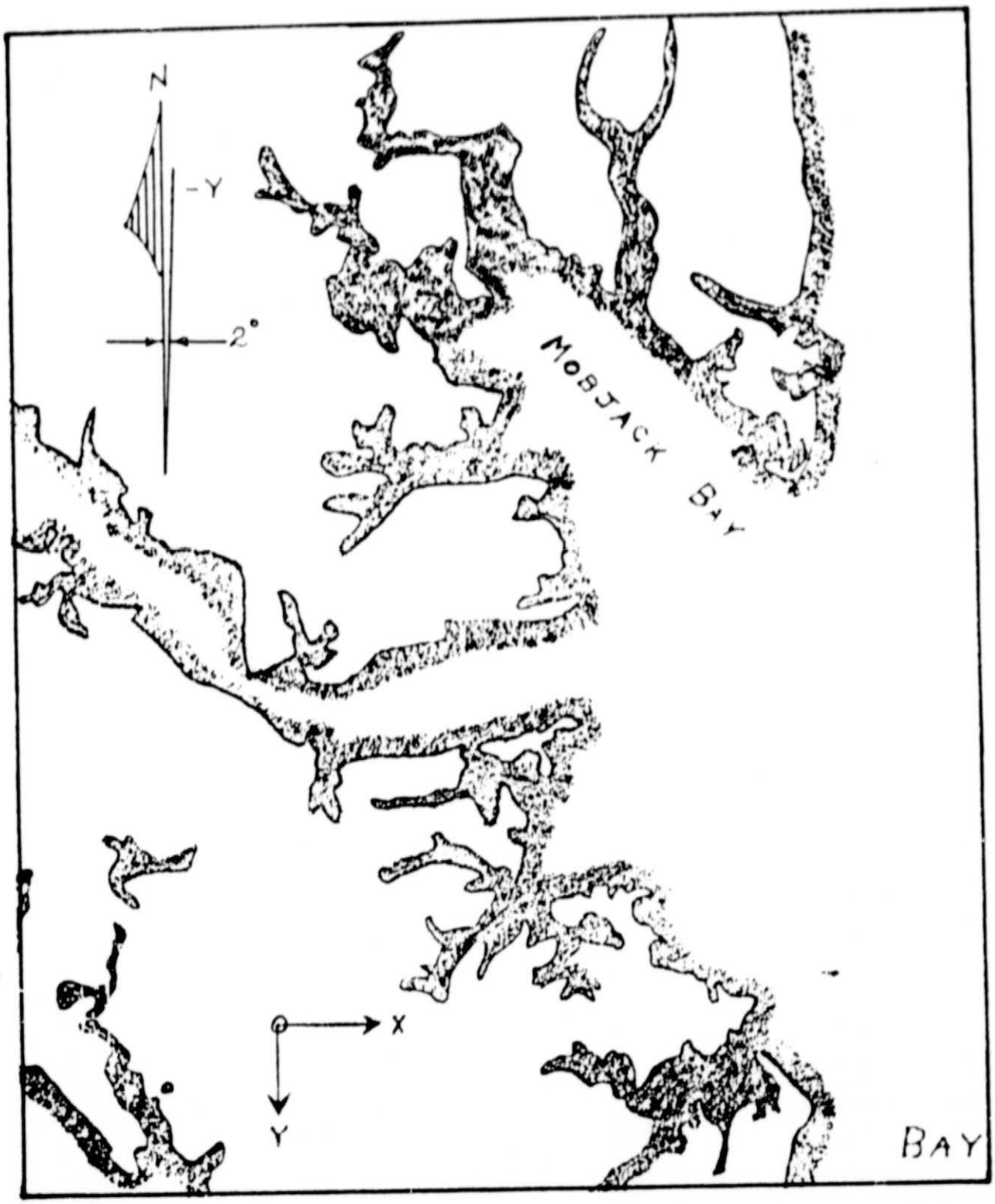

Figure 5.12 Topographical Map Showing Approaches to Runway 20.

to 3° and 6°; however, this has not been done at this time. The overlays, Figures 5.2, 5.5, 5.8 and 5.11 can be used to show the ground tracks for the eight trajectories. The steeper six-degree glide slope benefits first from the fact that less thrust is required to maintain the specified velocity and therefore less noise is generated by the engines. Secondly, the fact that the steeper trajectory is higher above the ground also causes the footprint to be generally smaller. These factors result in a ground track for the six-degree approach which is shorter and more narrow than that for the three-degree approach.

Besides the ground track itself, the intersection of it with the population model is also of vital significance. The second overlays, Figures 5.1, 5.4, 5.7 and 5.10 demonstrate this feature. It is seen that the approach along runway 24 spends a good deal of time over the Chesapeake Bay and over the rural areas to the northeast. The approach along runway 20 spends most of its time over the northern rural areas. These two approaches therefore influence fewer people than do the approaches along runways 6 and 2. All of these factors are reflected in the values of the performance index for the runs which are:

Runway 6	6° glide slope	PI = 16.1
Runway 6	3° glide slope	PI = 23.5
Runway 24	6° glide slope	PI = 9.2
Runway 24	3° glide slope	PI = 12.6
Runway 2	6° glide slope	PI = 19.8
Runway 2	3° glide slope	PI = 28.0
Runway 20	6° glide slope	PI = 9.2
Runway 20	3° glide slope	PI = 13.3

Runway 24 gives the best value for the performance index followed by runways 20, 6 and 2 in that order.

Printouts of the computer simulations are shown in Table I through 3. Table I is a glossary of input variables. In Tables 2 and 3 are given results for the approaches to runway 6. On the first three pages of

Table 5.1 Glossary of Input Variables

```
C.....
C.....
C.....                    READ INPUT DATA                              ...
C.....  TI AND TF ARE THE INITIAL AND FINAL TIMES                      ...
C.....  DT1 IS THE FORWARD INTEGRATION STEP SIZE                       ...
C.....  DT2 IS THE STATE VARIABLE PRINTOUT INTERVAL (INTEGER           ...
C.....      MULTIPLE OF DT4)                                          ...
C.....  DT3 IS THE INTERVAL FOR NOISE CONTOUR DETERMINATION           ...
C.....  DT4 IS THE TIME INTERVAL FOR BACKWARD INTEGRATION OF ADJOINT   ...
C.....      EQUATIONS. ALSO THE INTERVAL OF STORAGE OF STATE AND       ...
C.....      CONTROL VARIABLES (LESS THAN OR EQUAL TO DT2)              ...
C.....  YE AND ZE ARE THE HORIZONTAL AND VERTICAL MOMENT ARMS OF THE   ...
C.....     ENGINES ABOUT THE A/C CG                                    ...
C.....  CBAR IS MEAN CHORD LENGTH OF WING                             ...
C.....  S IS A/C WING AREA                                            ...
C.....  RIXX, RIYY, RIZZ AND RIXZ ARE THE A/C MOMENTS OF INERTIA      ...
C.....  WI IS THE A/C WEIGHT                                          ...
C.....  CG IS THE POSITION OF THE A/C CENTER OF GRAVITY (IN PERCENT    ...
C.....      OF CBAR)                                                  ...
C.....  B IS THE WING SPAN OF THE A/C                                 ...
C.....  GNMAX MAXIMUM DESIRED RATE OF CLIMB (LESS THAN OR EQUAL TO    ...
C.....      100 FEET/SEC)                                             ...
C.....  GNMIN MAXIMUM DESIRED RATE OF DESCENT (LESS THAN OR EQUAL TO  ...
C.....      250 FEET/SEC)                                             ...
C.....  HMIN IS THE MINIMUM DESIRED A/C ALTITUDE PERMISS  . (GREATER  ...
C.....      THAN 100 FEET)                                            ...
C.....  RANGE IS THE DISTANCE ALONG  X GROUND AXIS OF /  . AT TI      ...
C.....  SIDE IS THE DISTANCE ALONG Y GROUND AXIS OF A/C AT TI         ...
C.....  ALT IS THE MEAN SEA LEVEL ALTITUDE OF THE A/C AT TI           ...
C.....  PHI IS THE ROLL ANGLE OF THE A/C AT TI                        ...
C.....  THETA IS THE PITCH ANGLE OF A/C AT TI                         ...
C.....  PSI IS THE YAW ANGLE OF THE A/C AT TI                         ...
C.....  V IS THE VELOCITY (RELATIVE TO THE WIND) OF THE A/C AT TI     ...
C.....  P, Q AND R ARE THE ROLL, PITCH AND YAW RATES OF THE A/C AT TI ...
C.....  DALDT AND DBDT ARE THE RATES OF CHANGE OF THE ANGLE OF       ...
C.....      ATTACK AND SIDESLIP OF THE A/C AT TI                      ...
C.....  LIFT IS THE LIFT FORCE ON THE A/C AT TI                       ...
C.....  RNZ IS THE LOAD FACTOR AT TI                                  ...
C.....  ALPH AND BT ARE THE ANGLE OF ATTACK AND SIDESLIP ANGLES AT TI ...
C.....  XF IS THE DESIRED X-GROUND COORDINATE OF A/C AT TF            ...
C.....  YF IS THE DESIRED Y-GROUND COORDINATE OF A/C AT TF            ...
C.....  HF IS THE DESIRED MEAN SEA LEVEL ALTITUDE OF A/C AT TF       ...
C.....  VF IS THE DESIRED VELOCITY OF A/C AT TF                       ...
C.....  PHIF IS THE DESIRED ROLL ANGLE OF A/C AT TF                   ...
C.....  PSIF IS THE DESIRED YAW ANGLE OF A/C AT TF                    ...
C.....  THETAF IS THE DESIRED PITCH ANGLE OF A/C AT TF                ...
C.....  PF IS THE DESIRED ROLL RATE OF A/C AT TF                      ...
C.....  QF IS THE DESIRED PITCH RATE OF A/C AT TF                     ...
C.....  RF IS THE DESIRED YAW RATE OF A/C AT TF                       ...
C.....  GF IS THE DESIRED GLIDE SLOPE OF TRAJECTORY AT TF             ...
C.....  BF IS THE DESIRED SIDESLIP ANGLE OF A/C AT TF                 ...
C.....  XR IS THE X-GROUND COORDINATE OF THE RUNWAY EDGE              ...
C.....  YR IS THE Y-GROUND COORDINATE OF THE RUNWAY EDGE              ...
C.....  HD IS THE A/C ALTITUDE GREATER THAN DESIRED TERMINAL ALTITUDE ...
C.....      BUT LESS THAN ANY OPTIMAL TRAJECTORY WHICH PENETRATES      ...
C.....      WITHIN RF OF RUNWAY                                       ...
C.....  UP2 IS THE MAXIMUM FRACTION SPANNED OF PERTURBED CONTROL      ...
C.....      THAT IS TO BE UTILIZED                                    ...
C.....  APSI(12) IS THE MATRIX OF CONSTRAINT EQUATION COEFFICIENTS    ...
C.....      FOR THE CORRESPONDING STATE VARIABLES                     ...
C.....  WIA) CONTAINS THE DIAGONAL ELEMENTS OF THE CONTROL WEIGHTING  ...
C.....      MATRIX (NO ELEMENT CAN BE ZERO OR NEGATIVE)               ...
C.....  PLONG AND PLAT ARE THE POPULATION MODEL STANDARD RECTANGLE    ...
C.....      LENGTHS PARALLEL TO THE X AND Y GROUND AXES               ...
C.....  RA AND CA ARE THE ROW AND COLUMN VALUES OF THE POPULATION     ...
C.....      ARRAY WHICH IDENTIFIES THE GROUND SYSTEM ORIGIN           ...
C.....  KOPT(5) IS THE MATRIX OF PERFORMANCE INDEX COEFFICIENTS FOR   ...
C.....      1. FUEL  2. TIME  3. POPULATION                           ...
C.....  RHO IS THE FRACTION OF DPSI WHICH IS TO BE ELIMINATED ON      ...
C.....      EACH SUCCESSIVE ITERATION                                 ...
C.....  DT5 IS THE GROUND TRACK PRINTOUT INTERVAL (INTEGER MULTIPLE   ...
C.....      OF DT4                                                    ...
C.....  RIOPT (=0) OPTIMIZATION PERFORMED, (=-1) NO OPTIMIZATION      ...
C.....
C.....
```

Table 5.2 Simulation Printout for 3° Glide Slope Into Runway 6

****
****
** **
** INPUT DATA **
** **
****
****

TI (SEC)	TF (SEC)	DT1 (SEC)	DT2 (SEC)	DT3 (SEC)
0.000	600.000	.100	20.000	1.000

DT4 (SEC)	YE (FEET)	ZE (FEET)	CBAR (FEET)	S (SQ.FT)
20.000	16.200	5.000	11.200	980.000

RIXX (SQ.FT.-SLUG)	RIYY (SQ.FT.-SLUG)	RIZZ (SQ.FT.-SLUG)	RIXZ (SQ.FT.-SLUG)	W1 (LBS)
375000.0	875000.0	1200000.0	48000.0	90000.0

DT5 (SEC)	B (FEET)	DHMAX (FT/SEC)	DHMIN (FT/SEC)	HMIN (FEET)
10.000	93.0	100.0	250.0	100.0

RANGE (FEET)	SIDE (FEET)	ALT (FEET)	PHI (DEG)	THETA (DEG)
-87786.0	45832.0	4794.0	0.00	1.36

PSI (DEG)	V (FT/SEC)	P (RAD/SEC)	Q (RAD/SEC)	R (RAD/SEC)
-27.00	218.20	0.00	0.0000	0.0000

DA1DT (RAD/SEC)	DB1DT (RAD/SEC)	LIFT (LBS)	RNZ	AFRL (DEG)
0.0000	0.0000	90356.7	1.000	4.36

Table 5.2 (Continued)

****
INPUT DATA
****

B1 (DEG)	XF (FEET)	YF (FEET)	HF (FEET)	VF (FT/SEC)
0.00	-7510.0	4924.0	383.0	203.70

PHIF (DEG)	PSIF (DEG)	THETAF (DEG)	PF (RAD/SEC)	QF (RAD/SEC)
0.00	-27.00	1.36	0.0000	0.0000

RF (FEET)	GF (DEG)	UF (DEG)	XR (FEET)	YR (FEET)
.0000	-2.75	0.00	-1169.0	1693.0

PLONG (FEET)	PLAT (FEET)	HD (FEET)	RHO	UP2
5683.00	4877.00	5000.0	.500	10000.0

KPSI(1)	KPSI(2)	KPSI(3)	KPSI(4)	KPSI(5)
.10000E-01	.40000E+03	0.	.75000E+06	0.

KPSI(6)	KPSI(7)	KPSI(8)	KPSI(9)	KPSI(10)
.15000E+07	.50000E+05	0.	.15000E+05	.20000E-03

KPSI(11)	KPSI(12)	W(1)	W(2)	W(3)
.20000E-03	.30000E-02	.10000E+01	.10000E+01	.10000E+01

Table 5.2 (Continued)

****
INPUT DATA
****

W(4)	W(5)	W(6)	W(7)	W(8)
.10000E+01	.10000E+01	.10000E+01	.10000E+01	.10000E+01

KOPT(1)	KOPT(2)	KOPT(3)	RA	CA
.50000E-02	.70000E-02	.10000E-03	24.	21.

CG	RIOPT
.200	-1.0

Table 5.2 (Continued)

****
****
** **
** TRAJECTORY DATA **
** **
****
****

TIME (SEC)	GLIDE SLOPE (DEG)	AIRCRAFT VELOCITY (FT/SEC)	ANGLE OF ATTACK (RAD)	SIDESLIP ANGLE (RAD)
ROLL RATE (RAD/SEC)	PITCH RATE (RAD/SEC)	YAW RATE (RAD/SEC)	YAW ANGLE (RAD)	PITCH ANGLE (RAD)
ROLL ANGLE (RAD)	X-GROUND COORDINATE (FEET)	Y-GROUND COORDINATE (FEET)	ALTITUDE (FEET)	PERFORMANCE INDEX (J)
AREA-TIME SUM (MI**2-SEC)	PEOPLE-TIME SUM (PEOPLE-SEC)	INSTANT. NOISE-AREA (SQ.MI.)	INSTANT. NOISE-PEOPLE (PEOPLE)	TIME J-COMPONENT (SEC)
FUEL J-COMPONENT (LBS)	PEOPLE J-COMPONENT (PEOPLE-SEC)			

Table 5.2 (Continued)

0.	-.3000000E+01	.2182000E+03	.7609287E-01	0.
0.	0.	0.	-.4712389E+00	.2373299E-01
0.	-.8778600E+05	.4583200E+05	.4794000E+04	0.
0.	0.	.3022551E+01	.6468238E+02	0.
0.	0.			
.2000000E+02	-.2649399E+01	.2199558E+03	.6492571E-01	0.
0.	.1049570E-02	0.	-.4712389E+00	.1868497E-01
0.	-.8388011E+05	.4384185E+05	.4562148E+04	.4286652E+00
.6117709E+02	.1302938E+04	.3087714E+01	.6580314E+02	.1400000E+00
.1583684E+00	.1302938E+00			
.4000000E+02	-.2959354E+01	.2175621E+03	.6610152E-01	0.
0.	-.6853647E-03	0.	-.4712389E+00	.1445105E-01
0.	-.7999503E+05	.4186230E+05	.4362316E+04	.8616547E+00
.1232978E+03	.2649061E+04	.3129666E+01	.6857533E+02	.2800000E+00
.3167369E+00	.2649061E+00			
.6000000E+02	-.2628642E+01	.2178272E+03	.6548216E-01	0.
0.	.3945572E-03	0.	-.4712389E+00	.1960370E-01
0.	-.7611217E+05	.3988389E+05	.4141852E+04	.1302072E+01
.1861824E+03	.4069396E+04	.3154078E+01	.7331042E+02	.4200000E+00
.4751053E+00	.4069396E+00			
.8000000E+02	-.2933479E+01	.2166806E+03	.6575162E-01	0.
0.	-.1801077E-03	0.	-.4712389E+00	.1455275E-01
0.	-.7225224E+05	.3791716E+05	.3934922E+04	.1745357E+01
.2494115E+03	.5518606E+04	.3168878E+01	.7182979E+02	.5600000E+00
.6334738E+00	.5518606E+00			

Table 5.2 (Continued)

.1000000E+03	-.2680238E+01	.2160855E+03	.6576005E-01	0.
0.	.3754246E-04	0.	-.4712389E+00	.1898107E-01
0.	-.6839542E+05	.3595201E+05	.3722085E+04	.2188055E+01
.3127578E+03	.6961861E+04	.3162063E+01	.7325521E+02	.7000000E+00
.7918422E+00	.6961861E+00			
.1200000E+03	-.2873311E+01	.2155108E+03	.6563866E-01	0.
0.	.5168180E-04	0.	-.4712389E+00	.1548993E-01
0.	-.6455835E+05	.3399692E+05	.3512106E+04	.2636074E+01
.3758689E+03	.8458277E+04	.3147132E+01	.7580325E+02	.8400000E+00
.9502106E+00	.8458277E+00			
.1400000E+03	-.2739796E+01	.2146099E+03	.6585488E-01	0.
0.	-.9383696E-04	0.	-.4712389E+00	.1803642E-01
0.	-.6072798E+05	.3204525E+05	.3303313E+04	.3084360E+01
.4384954E+03	.9957509E+04	.3111797E+01	.7401214E+02	.9800000E+00
.1108579E+01	.9957509E+00			
.1600000E+03	-.2822519E+01	.2141815E+03	.6565776E-01	0.
0.	.1074133E-03	0.	-.4712389E+00	.1639552E-01
0.	-.5691338E+05	.3010161E+05	.3093159E+04	.3529654E+01
.5003498E+03	.1142681E+05	.3066746E+01	.7246150E+02	.1120000E+01
.1266948E+01	.1142681E+01			
.1800000E+03	-.2780602E+01	.2132772E+03	.6586183E-01	0.
0.	-.9870823E-04	0.	-.4712389E+00	.1733117E-01
0.	-.5310864E+05	.2816300E+05	.2886205E+04	.3967589E+01
.5611766E+03	.1282268E+05	.3009669E+01	.6587048E+02	.1260000E+01
.1425316E+01	.1282268E+01			

Table 5.2 (Continued)

.2000000E+03	-.2794179E+01	.2128000E+03	.6572645E-01	0.
0.	.8132245E-04	0.	-.4712389E+00	.1695883E-01
0.	-.4931682E+05	.2623097E+05	.2677376E+04	.4374754E+01
.6207513E+03	.1391146E+05	.2940720E+01	.3839295E+02	.1400000E+01
.1583684E+01	.1391146E+01			

.2200000E+03	-.2799276E+01	.2119995E+03	.6584699E-01	0.
0.	-.5793893E-04	0.	-.4712389E+00	.1699041E-01
0.	-.4553662E+05	.2430486E+05	.2471301E+04	.4721915E+01
.6788034E+03	.1440030E+05	.2858987E+01	.1067342E+02	.1540000E+01
.1742053E+01	.1440030E+01			

.2400000E+03	-.2785029E+01	.2114310E+03	.6579632E-01	0.
0.	.3748280E-04	0.	-.4712389E+00	.1718840E-01
0.	-.4176789E+05	.2238460E+05	.2264264E+04	.5026844E+01
.7350693E+03	.1446629E+05	.2762060E+01	0.	.1680000E+01
.1900421E+01	.1446629E+01			

.2600000E+03	-.2802859E+01	.2107318E+03	.6584277E-01	0.
0.	-.1841794E-04	0.	-.4712389E+00	.1692364E-01
0.	-.3801131E+05	.2047053E+05	.2058898E+04	.5325213E+01
.7893484E+03	.1446629E+05	.2657903E+01	0.	.1820000E+01
.2058790E+01	.1446629E+01			

.2800000E+03	-.2786445E+01	.2101006E+03	.6584896E-01	0.
0.	.6280039E-05	0.	-.4712389E+00	.1721631E-01
0.	-.3426575E+05	.1856207E+05	.1853569E+04	.5623581E+01
.8413912E+03	.1446629E+05	.2539202E+01	0.	.1960000E+01
.2217158E+01	.1446629E+01			

Table 5.2 (Continued)

.3000000E+03	-.2799956E+01	.2094619E+03	.6585657E-01	0.
0.	.3255347E-05	0.	-.4712389E+00	.1698811E-01
0.	-.3053215E+05	.1665971E+05	.1649082E+04	.5921949E+01
.8909818E+03	.1446629E+05	.2412387E+01	0.	.2100000E+01
.2375527E+01	.1446629E+01			
.3200000E+03	-.2790923E+01	.2088097E+03	.6588467E-01	0.
0.	-.6465198E-05	0.	-.4712389E+00	.1717387E-01
0.	-.2680959E+05	.1476297E+05	.1445213E+04	.6220318E+01
.9379005E+03	.1446629E+05	.2270733E+01	0.	.2240000E+01
.2533895E+01	.1446629E+01			
.3400000E+03	-.2796427E+01	.2081943E+03	.6588317E-01	0.
0.	.8759701E-05	0.	-.4712389E+00	.1707632E-01
0.	-.2309857E+05	.1287211E+05	.1241814E+04	.6520181E+01
.9819481E+03	.1448102E+05	.2123306E+01	.1267435E+02	.2380000E+01
.2692263E+01	.1448102E+01			
.3600000E+03	-.2794420E+01	.2075494E+03	.6591094E-01	0.
0.	-.6858495E-05	0.	-.4712389E+00	.1713911E-01
0.	-.1939866E+05	.1098691E+05	.1039200E+04	.7016730E+01
.1022904E+04	.1645606E+05	.1963206E+01	.2535238E+03	.2520000E+01
.2850632E+01	.1645606E+01			
.3800000E+03	-.2794622E+01	.2069381E+03	.6591464E-01	0.
0.	.6120406E-05	0.	-.4712389E+00	.1713928E-01
0.	-.1570993E+05	.9107407E+04	.8370082E+03	.8874034E+01
.1060581E+04	.3200364E+05	.1794349E+01	.1661777E+04	.2660000E+01
.3009000E+01	.3200364E+01			

Table 5.2 (Continued)

.4000000E+03	-.2795972E+01	.2063106E+03	.6593475E-01	0.
0.	-.2935680E-05	0.	-.4712389E+00	.1713583E-01
0.	-.1203228E+05	.7233551E+04	.6355491E+03	.1445445E+02
.1094785E+04	.8475923E+05	.1615103E+01	.3655938E+04	.2800000E+01
.3167369E+01	.8475923E+01			

.4200000E+03	-.2794510E+01	.2056998E+03	.6594560E-01	0.
0.	.2165421E-05	0.	-.4712389E+00	.1717219E-01
0.	-.8365573E+04	.5365271E+04	.4345883E+03	.2205985E+02
.1125329E+04	.1578411E+06	.1428474E+01	.3080566E+04	.2940000E+01
.3325737E+01	.1578411E+02			

.4247000E+03	-.2794556E+01	.2055536E+03	.6595074E-01	0.
0.	-.2973261E-06	0.	-.4712389E+00	.1717654E-01
0.	-.7505488E+04	.4927036E+04	.3874707E+03	.2349806E+02
.1131954E+04	.1715387E+06	0.	0.	.2972900E+01
.3362954E+01	.1715387E+02			

Table 5.2 (Continued)

NOISE CONTOUR GROUND TRACK (QUADRANT 4)

XMAX	YMAX	XMIN	YMIN
-.91173E+02	.41600E+02	-.92237E+02	.48100E+02
-.89231E+02	.40600E+02	-.82817E+02	.43500E+02
-.87287E+02	.39600E+02	-.80656E+02	.42200E+02
-.85331E+02	.38600E+02	-.78695E+02	.41200E+02
-.83371E+02	.37600E+02	-.76733E+02	.40200E+02
-.81404E+02	.36600E+02	-.74770E+02	.39200E+02
-.79431E+02	.35600E+02	-.72611E+02	.38100E+02
-.77454E+02	.34600E+02	-.70648E+02	.37100E+02
-.75469E+02	.33600E+02	-.68686E+02	.36100E+02
-.73673E+02	.32700E+02	-.66723E+02	.35100E+02
-.71678E+02	.31700E+02	-.64761E+02	.34100E+02
-.69679E+02	.30700E+02	-.62798E+02	.33100E+02
-.67671E+02	.29700E+02	-.60835E+02	.32100E+02
-.65854E+02	.28800E+02	-.58873E+02	.31100E+02
-.63838E+02	.27800E+02	-.56910E+02	.30100E+02
-.61815E+02	.26800E+02	-.55144E+02	.29200E+02
-.59983E+02	.25900E+02	-.53181E+02	.28200E+02
-.57948E+02	.24900E+02	-.51219E+02	.27200E+02
-.56107E+02	.24000E+02	-.49256E+02	.26200E+02
-.54061E+02	.23000E+02	-.47490E+02	.25300E+02
-.52208E+02	.22100E+02	-.45527E+02	.24300E+02
-.50348E+02	.21200E+02	-.43564E+02	.23300E+02
-.48288E+02	.20200E+02	-.41798E+02	.22400E+02
-.46418E+02	.19300E+02	-.39836E+02	.21400E+02
-.44541E+02	.18400E+02	-.37873E+02	.20400E+02
-.42659E+02	.17500E+02	-.36107E+02	.19500E+02
-.40575E+02	.16500E+02	-.34144E+02	.18500E+02
-.38682E+02	.15600E+02	-.32378E+02	.17600E+02
-.36783E+02	.14700E+02	-.30415E+02	.16600E+02
-.34878E+02	.13800E+02	-.28649E+02	.15700E+02
-.32965E+02	.12900E+02	-.26882E+02	.14800E+02
-.31046E+02	.12000E+02	-.24920E+02	.13800E+02
-.29120E+02	.11100E+02	-.23153E+02	.12900E+02
-.27187E+02	.10200E+02	-.21387E+02	.12000E+02
-.25245E+02	.93000E+01	-.19424E+02	.11000E+02
-.23493E+02	.85000E+01	-.17658E+02	.10100E+02
-.21538E+02	.76000E+01	-.15892E+02	.92000E+01
-.19573E+02	.67000E+01	-.14125E+02	.83000E+01
-.17597E+02	.58000E+01	-.12359E+02	.74000E+01
-.15811E+02	.50000E+01	-.10593E+02	.65000E+01
-.13817E+02	.41000E+01	-.88263E+01	.56000E+01
-.12008E+02	.33000E+01	-.70599E+01	.47000E+01
-.99897E+01	.24000E+01	-.52936E+01	.38000E+01
-.90817E+01	.20000E+01	-.45085E+01	.34000E+01

Table 5.2 (Continued)

NOISE CONTOUR GROUND TRACK (QUADRANT 3)

XMAX	YMAX	XMIN	YMIN
-.86433E+02	.51100E+02	-.92237E+02	.48100E+02
-.84448E+02	.50100E+02	-.82817E+02	.43300E+02
-.82468E+02	.49100E+02	-.80658E+02	.42200E+02
-.80498E+02	.48100E+02	-.78695E+02	.41200E+02
-.78533E+02	.47100E+02	-.76733E+02	.40200E+02
-.76575E+02	.46100E+02	-.74770E+02	.39200E+02
-.74623E+02	.45100E+02	-.72611E+02	.38100E+02
-.72675E+02	.44100E+02	-.70648E+02	.37100E+02
-.70733E+02	.43100E+02	-.68686E+02	.36100E+02
-.68800E+02	.42100E+02	-.66723E+02	.35100E+02
-.66871E+02	.41100E+02	-.64761E+02	.34100E+02
-.64945E+02	.40100E+02	-.62798E+02	.33100E+02
-.63027E+02	.39100E+02	-.60835E+02	.32100E+02
-.61116E+02	.38100E+02	-.58873E+02	.31100E+02
-.59208E+02	.37100E+02	-.56910E+02	.30100E+02
-.57305E+02	.36100E+02	-.55144E+02	.29200E+02
-.55213E+02	.35000E+02	-.53181E+02	.28200E+02
-.53321E+02	.34000E+02	-.51219E+02	.27200E+02
-.51433E+02	.33000E+02	-.49256E+02	.26200E+02
-.49552E+02	.32000E+02	-.47490E+02	.25300E+02
-.47678E+02	.31000E+02	-.45527E+02	.24300E+02
-.45808E+02	.30000E+02	-.43564E+02	.23300E+02
-.43943E+02	.29000E+02	-.41798E+02	.22400E+02
-.42086E+02	.28000E+02	-.39836E+02	.21400E+02
-.40234E+02	.27000E+02	-.37873E+02	.20400E+02
-.38189E+02	.25900E+02	-.36107E+02	.19500E+02
-.36347E+02	.24900E+02	-.34144E+02	.18500E+02
-.34511E+02	.23900E+02	-.32378E+02	.17600E+02
-.32682E+02	.22900E+02	-.30415E+02	.16600E+02
-.30860E+02	.21900E+02	-.28649E+02	.15700E+02
-.28848E+02	.20800E+02	-.26882E+02	.14800E+02
-.27037E+02	.19800E+02	-.24920E+02	.13800E+02
-.25233E+02	.18800E+02	-.23153E+02	.12900E+02
-.23438E+02	.17800E+02	-.21387E+02	.12000E+02
-.21455E+02	.16700E+02	-.19424E+02	.11000E+02
-.19672E+02	.15700E+02	-.17658E+02	.10100E+02
-.17899E+02	.14700E+02	-.15892E+02	.92000E+01
-.16137E+02	.13700E+02	-.14125E+02	.83000E+01
-.14185E+02	.12600E+02	-.12359E+02	.74000E+01
-.12439E+02	.11600E+02	-.10593E+02	.65000E+01
-.10510E+02	.10500E+02	-.88263E+01	.56000E+01
-.87843E+01	.95000E+01	-.70599E+01	.47000E+01
-.70755E+01	.85000E+01	-.52936E+01	.38000E+01
-.62160E+01	.80000E+01	-.45085E+01	.34000E+01

Table 5.3 Simulation Printout for 6° Glide Slope Into Runway 6

****
****
** INPUT DATA **
****
****

TI (SEC)	TF (SEC)	DT1 (SEC)	DT2 (SEC)	DT3 (SEC)
0.000	600.000	.100	20.000	1.000

DT4 (SEC)	YE (FEET)	ZE (FEET)	CBAR (FEET)	S (SQ.FT.)
20.000	16.200	5.000	11.200	980.000

RIXX (SQ.FT.-SLUG)	RIYY (SQ.FT.-SLUG)	RIZZ (SQ.FT.-SLUG)	RIXZ (SQ.FT.-SLUG)	W1 (LBS)
375000.0	875000.0	1200000.0	48000.0	90000.0

DT5 (SEC)	B (FEET)	DHMAX (FT/SEC)	DHMIN (FT/SEC)	HMIN (FEET)
10.000	93.0	100.0	250.0	100.0

RANGE (FEET)	SIDE (FEET)	ALT (FEET)	PHI (DEG)	THETA (DEG)
-87786.0	45832.0	9623.0	0.00	-4.28

PSI (DEG)	V (FT/SEC)	P (RAD/SEC)	Q (RAD/SEC)	R (RAD/SEC)
-27.00	253.50	0.00	0.0000	0.0000

DA1DT (RAD/SEC)	DB1DT (RAD/SEC)	LIFT (LBS)	RNZ	AFRL (DEG)
0.0000	0.0000	89751.0	1.000	1.72

Table 5.3 (Continued)

****
****
** **
** INPUT DATA **
** **
****
****

B1 (DEG)	XF (FEET)	YF (FEET)	HF (FEET)	VF (FT/SEC)
0.00	-7510.0	4924.0	383.0	220.60

PHIF (DEG)	PSIF (DEG)	THETAF (DEG)	PF (RAD/SEC)	QF (RAD/SEC)
0.00	-27.00	-4.28	0.0000	0.0000

RF (FEET)	GF (DEG)	BF (DEG)	XR (FEET)	YR (FEET)
0.0000	-2.75	0.00	-1169.0	1693.0

PLONG (FEET)	PLAT (FEET)	HO (FEET)	RHO	DP2
5683.00	4877.00	5000.0	.500	10000.0

KPSI(1)	KPSI(2)	KPSI(3)	KPSI(4)	KPSI(5)
.10000E-01	.40000E+03	0.	.75000E+06	0.

KPSI(6)	KPSI(7)	KPSI(8)	KPSI(9)	KPSI(10)
.15000E+07	.50000E+05	0.	.15000E+05	.20000E-03

KPSI(11)	KPSI(12)	W(1)	W(2)	W(3)
.20000E-03	.30000E-02	.10000E+01	.10000E+01	.10000E+01

Table 5.3 (Continued)

****
INPUT DATA
****

W(4)	W(5)	W(6)	W(7)	W(8)
.10000E+01	.10000E+01	.10000E+01	.10000E+01	.10000E+01

KOPT(1)	KOPT(2)	KOPT(3)	RA	CA
.50000E-02	.70000E-02	.10000E-03	24.	21.

CG	RIOPT
.300	-1.0

Table 5.3 (Continued)

****
****
** TRAJECTORY DATA **
****
****

TIME (SEC)	GLIDE SLOPE (DEG)	AIRCRAFT VELOCITY (FT/SEC)	ANGLE OF ATTACK (RAD)	SIDESLIP ANGLE (RAD)
ROLL RATE (RAD/SEC)	PITCH RATE (RAD/SEC)	YAW RATE (RAD/SEC)	YAW ANGLE (RAD)	PITCH ANGLE (RAD)
ROLL ANGLE (RAD)	X-GROUND COORDINATE (FEET)	Y-GROUND COORDINATE (FEET)	ALTITUDE (FEET)	PERFORMANCE INDEX (J)
AREA-TIME SUM (MI**2-SEC)	PEOPLE-TIME SUM (PEOPLE-SEC)	INSTANT. NOISE-AREA (SQ.MI.)	INSTANT. NOISE-PEOPLE (PEOPLE)	TIME J-COMPONENT (SEC)
FUEL J-COMPONENT (LBS)	PEOPLE J-COMPONENT (PEOPLE-SEC)			

Table 5.3 (Continued)

```
 0.              -.5999950E+01   .2535000E+03   .3005544E-01   0.
 0.              0.              0.             -.4712389E+00  -.7466344E-01
 0.              -.8778600E+05   .4583200E+05   .9623000E+04   0.
 0.              0.              0.             0.             0.
 0.              0.

 .2000000E+02    -.5850788E+01   .2535541E+03   .2870259E-01   0.
 0.               .5865771E-03   0.             -.4712389E+00  -.7341292E-01
 0.              -.8328841E+05   .4354037E+05   .9088683E+04    .2336495E+00
 0.              0.              0.             0.              .1400000E+00
  .9364950E-01   0.

 .4000000E+02    -.5755711E+01   .2498075E+03   .3000177E-01   0.
 0.              -.3626713E-03   0.             -.4712389E+00  -.7045435E-01
 0.              -.7882579E+05   .4126655E+05   .8588734E+04    .4672990E+00
 0.              0.              0.             0.              .2800000E+00
  .1872990E+00   0.

 .6000000E+02    -.5942634E+01   .2487801E+03   .2936628E-01   0.
 0.               .1817881E-03   0.             -.4712389E+00  -.7435225E-01
 0.              -.7440938E+05   .3901627E+05   .8075204E+04    .7009485E+00
 0.              0.              0.             0.             -.4200000E+00
  .2809485E+00   0.

 .8000000E+02    -.5750467E+01   .2463001E+03   .2987454E-01   0.
 0.              -.3279655E-04   0.             -.4712389E+00  -.7049005E-01
 0.              -.7001784E+05   .3677867E+05   .7573287E+04    .9345980E+00
 0.              0.              0.             0.              .5600000E+00
  .3745980E+00   0.
```

Table 5.3 (Continued)

```
 .1000000E+03  -.5907846E+01   .2444266E+03   .2989283E-01  0.
 0.            -.3424615E-04   0.             -.4712389E+00  -.7321854E-01
 0.            -.6567103E+05    .3456386E+05   .7074555E+04   .1168248E+01
 0.            0.              0.             0.             .7000000E+00
  .4682475E+00  0.

 .1200000E+03  -.5801244E+01   .2426100E+03   .2995804E-01  0.
 0.             .7865737E-04   0.             -.4712389E+00  -.7129277E-01
 0.            -.6135206E+05    .3236324E+05   .6576995E+04   .1409040E+01
  .2964635E+01  .7111096E+02   .4667567E+00   .1097570E+02   .8400000E+00
  .5618970E+00  .7111096E-02

 .1400000E+03  -.5863254E+01   .2405165E+03   .3021266E-01  0.
 0.            -.7077953E-04   0.             -.4712389E+00  -.7212043E-01
 0.            -.5707103E+05    .3018194E+05   .6087262E+04   .1678629E+01
  .1818223E+02  .4300409E+03   .1071263E+01   .2551677E+02   .9800000E+00
  .6555465E+00  .4300409E-01

 .1600000E+03  -.5836619E+01   .2388618E+03   .3018580E-01  0.
 0.             .7011146E-04   0.             -.4712389E+00  -.7168243E-01
 0.            -.5282137E+05    .2801663E+05   .5597478E+04   .1974446E+01
  .4466186E+02  .1051387E+04   .1588083E+01   .3523328E+02   .1120000E+01
  .7491960E+00  .1051387E+00

 .1800000E+03  -.5841946E+01   .2368666E+03   .3043329E-01  0.
 0.            -.4189983E-04   0.             -.4712389E+00  -.7152791E-01
 0.            -.4860486E+05    .2586821E+05   .5114464E+04   .2275260E+01
  .8046342E+02  .1723279E+04   .1976756E+01   .2543484E+02   .1260000E+01
  .8428455E+00  .1723279E+00
```

Table 5.3 (Continued)

```
 .2000000E+03  -.5849347E+01   .2352009E+03   .3045190E-01  0.
 0.            .3648177E-04  0.             -.4712389E+00  -.7163847E-01
 0.            -.4442067E+05   .2373626E+05   .4632967E+04   .2535893E+01
 .1222931E+03   .1993861E+04   .2195389E+01   .2987486E+01   .1400000E+01
 .9364950E+00   .1993861E+00

 .2200000E+03  -.5837787E+01   .2333615E+03   .3063345E-01  0.
 0.            -.1232736E-04  0.             -.4712389E+00  -.7125515E-01
 0.            -.4026733E+05   .2162003E+05   .4156372E+04   .2770636E+01
 .1674146E+03   .2004919E+04   .2307688E+01  0.             .1540000E+01
 .1030144E+01   .2004919E+00

 .2400000E+03  -.5850475E+01   .2316829E+03   .3070596E-01  0.
 0.            .1380855E-04  0.             -.4712389E+00  -.7140409E-01
 0.            -.3614554E+05   .1951987E+05   .3682598E+04   .3004286E+01
 .2139265E+03   .2004919E+04   .2334245E+01  0.             .1680000E+01
 .1123794E+01   .2004919E+00

 .2600000E+03  -.5839944E+01   .2299650E+03   .3083812E-01  0.
 0.            .2763908E-05  0.             -.4712389E+00  -.7108813E-01
 0.            -.3205347E+05   .1743486E+05   .3212577E+04   .3237935E+01
 .2603126E+03   .2004919E+04   .2290790E+01  0.             .1820000E+01
 .1217443E+01   .2004919E+00

 .2800000E+03  -.5848547E+01   .2283086E+03   .3093851E-01  0.
 0.            .4478599E-05  0.             -.4712389E+00  -.7113788E-01
 0.            -.2799164E+05   .1536525E+05   .2745910E+04   .3471585E+01
 .3052744E+03   .2004919E+04   .2189568E+01  0.             .1960000E+01
 .1311093E+01   .2004919E+00
```

Table 5.3 (Continued)

.3000000E+03 -.5842722E+01 .2266743E+03 .3104638E-01 0.
0. .7388856E-05 0. -.4712389E+00 -.7092035E-01
0. -.2395872E+05 .1331038E+05 .2282511E+04 .3705234E+01
.3476757E+03 .2004919E+04 .2033785E+01 0. .2100000E+01
.1404742E+01 .2004919E+00

.3200000E+03 -.5846917E+01 .2250636E+03 .3115387E-01 0.
0. .2366360E-05 0. -.4712389E+00 -.7089408E-01
0. -.1995476E+05 .1127025E+05 .1022522E+04 .4024273E+01
.3865176E+03 .2854787E+04 .1833641E+01 .1434571E+03 .2240000E+01
.1498392E+01 .2854787E+00

.3400000E+03 -.5844541E+01 .2234914E+03 .3125212E-01 0.
0. .7495426E-05 0. -.4712389E+00 -.7075436E-01
0. -.1597887E+05 .9244441E+04 .1365635E+04 .5176639E+01
.4209242E+03 .1201407E+05 .1590172E+01 .1121709E+04 .2380000E+01
.1592041E+01 .1201407E+01

.3600000E+03 -.5846138E+01 .2219350E+03 .3135695E-01 0.
0. .2721292E-05 0. -.4712389E+00 -.7067740E-01
0. -.1203080E+05 .7232799E+04 .9120365E+03 .9407635E+01
.4501387E+03 .5192931E+05 .1312848E+01 .2934370E+04 .2520000E+01
.1685691E+01 .5192931E+01

.3800000E+03 -.5845474E+01 .2204157E+03 .3145112E-01 0.
0. .6445343E-05 0. -.4712389E+00 -.7057166E-01
0. -.8109947E+04 .5235022E+04 .4614697E+03 .1542777E+02
.4735090E+03 .1098090E+06 .1006079E+01 .2234858E+04 .2660000E+01
.1779340E+01 .1098090E+02

Table 5.3 (Continued)

.3031000E+03	-.5845276E+01	.2201810E+03	.3146690E-01	0.
0.	.5935579E-05	0.	-.4712389E+00	-.7055241E-01
0.	-.7504620E+04	.4926593E+04	.3919179E+03	.1612364E+02
.4765730E+03	.1164225E+06	0.	0.	.2681700E+01
.1793856E+01	.1164225E+02			

Table 5.3 (Continued)

NOISE CONTOUR GROUND TRACK (QUADRANT 4)

XMAX	YMAX	XMIN	YMIN
-.66914E+02	.31500E+02	-.66514E+02	.31000E+02
-.65067E+02	.29700E+02	-.63778E+02	.31500E+02
-.63185E+02	.28400E+02	-.61485E+02	.30900E+02
-.61067E+02	.27100E+02	-.59042E+02	.30100E+02
-.59011E+02	.25900E+02	-.56731E+02	.29300E+02
-.56865E+02	.24700E+02	-.54313E+02	.28400E+02
-.54844E+02	.23600E+02	-.52169E+02	.27600E+02
-.52575E+02	.22400E+02	-.50826E+02	.27000E+02
-.50455E+02	.21300E+02	-.46116E+02	.24600E+02
-.48494E+02	.20300E+02	-.43761E+02	.23400E+02
-.46303E+02	.19200E+02	-.41209E+02	.22100E+02
-.44273E+02	.18200E+02	-.39050E+02	.21000E+02
-.42022E+02	.17100E+02	-.36695E+02	.19800E+02
-.39939E+02	.16100E+02	-.34536E+02	.18700E+02
-.37829E+02	.15100E+02	-.32181E+02	.17500E+02
-.35696E+02	.14100E+02	-.30022E+02	.16400E+02
-.33537E+02	.13100E+02	-.27864E+02	.15300E+02
-.31554E+02	.12200E+02	-.25901E+02	.14300E+02
-.29350E+02	.11200E+02	-.23742E+02	.13200E+02
-.27319E+02	.10300E+02	-.21583E+02	.12100E+02
-.25263E+02	.94000E+01	-.19621E+02	.11100E+02
-.22989E+02	.84000E+01	-.17658E+02	.10100E+02
-.20885E+02	.75000E+01	-.15695E+02	.91000E+01
-.18949E+02	.67000E+01	-.13733E+02	.81000E+01
-.16792E+02	.58000E+01	-.11770E+02	.71000E+01
-.14602E+02	.49000E+01	-.98076E+01	.61000E+01
-.12573E+02	.41000E+01	-.80412E+01	.52000E+01
-.10502E+02	.33000E+01	-.60786E+01	.42000E+01
-.91951E+01	.28000E+01	-.50973E+01	.37000E+01

Table 5.3 (Continued)

NOISE CONTOUR GROUND TRACK (QUADRANT 3)

XMAX	YMAX	XMIN	YMIN
-.63794E+02	.37300E+02	-.64016E+02	.36900E+02
-.61516E+02	.37000E+02	-.62214E+02	.34900E+02
-.59073E+02	.36100E+02	-.60189E+02	.33300E+02
-.56876E+02	.35200E+02	-.58115E+02	.31800E+02
-.54616E+02	.34200E+02	-.56110E+02	.30400E+02
-.52443E+02	.33200E+02	-.54013E+02	.29000E+02
-.50339E+02	.32200E+02	-.52038E+02	.27700E+02
-.48293E+02	.31200E+02	-.50826E+02	.27000E+02
-.46092E+02	.30100E+02	-.46116E+02	.24600E+02
-.43932E+02	.29000E+02	-.43761E+02	.23400E+02
-.41808E+02	.27900E+02	-.41406E+02	.22200E+02
-.39714E+02	.26800E+02	-.39050E+02	.21000E+02
-.37649E+02	.25700E+02	-.36695E+02	.19800E+02
-.35611E+02	.24600E+02	-.34536E+02	.18700E+02
-.33599E+02	.23500E+02	-.32181E+02	.17500E+02
-.31613E+02	.22400E+02	-.30022E+02	.16400E+02
-.29451E+02	.21200E+02	-.27864E+02	.15300E+02
-.27510E+02	.20100E+02	-.25901E+02	.14300E+02
-.25397E+02	.18900E+02	-.23742E+02	.13200E+02
-.23502E+02	.17800E+02	-.21583E+02	.12100E+02
-.21434E+02	.16600E+02	-.19621E+02	.11100E+02
-.19590E+02	.15500E+02	-.17658E+02	.10100E+02
-.17571E+02	.14300E+02	-.15695E+02	.91000E+01
-.15579E+02	.13100E+02	-.13733E+02	.81000E+01
-.13617E+02	.11900E+02	-.11770E+02	.71000E+01
-.11686E+02	.10700E+02	-.98076E+01	.61000E+01
-.97898E+01	.95000E+01	-.80412E+01	.52000E+01
-.79346E+01	.83000E+01	-.60786E+01	.42000E+01
-.66900E+01	.75000E+01	-.50973E+01	.37000E+01

Tables 2 and 3 the input data are printed as a check on the user's input accuracy. This is followed by a page of headers denoting the positions and dimensions of the output variables as they appear in the printout. Next are the printouts of the output variables themselves at twenty second intervals. The final two pages give the ground track coordinates in thousands of feet. Because all the 3° trajectories were similar only one set of printouts is given. The fuel, time and passenger comfort terms are identical. Only the noise term differs. The same is true also for the 6° trajectories.

The computer execution time averages sixty percent of real time i.e. to simulate a 400 second flight trajectory requires approximately 240 seconds of execution time. The cost of the 400 second flight is approximately twenty-five dollars. Our estimate of the execution time required for the backward integration required by the optimization procedure is twice that of the forward integration making the cost per iteration approximately seventy-five dollars.

It will be interesting to see how the optimum trajectories are influenced by factors such as rivers, spots of high population density, etc. The plots of the ground track should aid in these interpretations.

VI. Future Work

Now that all the various models required by the optimization procedure have been developed and tested the actual trajectory optimization can begin. Landing trajectories will be optimized for flights from Washington, D. C. Both the 60 degree and the 240 degree runway directions will be utilized. While the total computer program is enormous and quite expensive to run it is still hoped that some sensitivity studies can be made. Coefficients on the various terms in the performance index will be varied and also perhaps variations in the point at which the aircraft enters the near terminal area can be considered.

In addition to its use in the optimization studies it is hoped that the aircraft simulation and the performance measure will find application in evaluating and comparing non-optimal trajectories which for one reason or another may be worthy of consideration.

REFERENCES

1. Cook G., Witt, R. M. and Barkana, A., "Research Studies in the Area of Optimal Landing Flight Path Trajectories," NASA Contract No. NAS 1-10210, Task Order No. 8, UVA Report No. EE-4038-101-74.

2. Bryson, A. E. and Denham, W. F., "A Steepest-Ascent Method for Solving Optimum Programming Problems," ASME Journal of Applied Mechanics, June 1962, pp. 247-257.

3. Rosko, J. S., Digital Simulation of Physical Systems, Addison-Wesley Publishing Co., Reading, Massachusetts, 1972.

4. Price, M. G. and Cook, G., "Use of Padé Approximants to the Matrix Exponential for Computer Solutions of State Equations," submitted to IEEE Transactions on Automatic Control.

5. Jacobson, I. A. and Kuhlthau, A. R., "Determining STOL Ride Quality Criteria - Passenger Acceptance," AIAA Journal of Aircraft, Vol. 10, No. 3, March 1973, pp. 163-166.